Remote Sensing of Environment 304 (2024) 114069

Contents lists available at ScienceDirect

Remote Sensing of Environment

journal homepage: www.elsevier.com/locate/rse

National tree species mapping using Sentinel-1/2 time series and German National Forest Inventory data

Lukas Blickensdörfer [a,b,c,*], Katja Oehmichen [a], Dirk Pflugmacher [b], Birgit Kleinschmit [d], Patrick Hostert [b,e]

[a] Thünen Institute of Forest Ecosystems, Alfred-Moeller-Straße 1, 16225 Eberswalde, Germany
[b] Geography Department, Humboldt Universität zu Berlin, Unter den Linden 6, 10099 Berlin, Germany
[c] Thünen Institute of Farm Economics, Bundesallee 63, 38116 Braunschweig, Germany
[d] Geoinformation in Environmental Planning Lab, Technische Universität Berlin, Straße des 17. Juni 145, 12, 10623 Berlin, Germany
[e] Integrative Research Institute on Transformations of Human-Environment Systems (IRI THESys), 14 Humboldt Universität zu Berlin, Unter den Linden 6, 10099 Berlin, Germany

ARTICLE INFO

Editor: Marie Weiss

Keywords:
Temperate forests
Time series
Large-area mapping
Optical remote sensing
SAR
Mixed forests
Environmental conditions

ABSTRACT

Spatially explicit and detailed information on tree species composition is critical for forest management, nature conservation and the assessment of forest ecosystem services. In many countries, forest attributes are monitored regularly through sample-based forest inventories. In combination with satellite imagery, data from such forest inventories have a great potential for developing large-area tree species maps. Here, the high temporal resolution of Sentinel-1 and Sentinel-2 has been useful for extracting vegetation phenology, information that may also be valuable for improving forest tree species mapping.

The objective of this study was to map the main tree species in Germany using combined Sentinel-1 and Sentinel-2 time series, and to identify and address challenges related to the use of National Forest Inventory (NFI) data in remote sensing applications. We generated cloud free time series with 5-day intervals from Sentinel-2 imagery and combine those with monthly Sentinel-1 backscatter composites. Further, we incorporate information on topography, meteorology, and climate to account for environmental gradients. To use NFI data for training machine learning models, we address the following challenges: 1) link satellite pixels with variable radius NFI plots, for which the precise area is unknown, and 2) efficiently utilize mixed-species NFI plots for model training and validation. In the past, accuracies for pixel-level species maps were often estimated solely for homogeneous pure-species stands. In this study, we assess how well pixel-level maps generalize to mixed plot conditions.

Our results show the potential of combined Sentinel-2 and Sentinel-1 time series with NFI data for tree species mapping in large, environmentally diverse landscapes. Classification accuracy in pure stands ranged between 72% and 97% (F1-score) for five dominant species, while mapping less frequent species remained challenging. When including mixed forest stands in the accuracy assessment, accuracy decreased by 4–14 percentage points for the most dominant species groups. Our study highlights the importance of including mixed-forest stands when training and validating tree species maps. Based on these results, we discuss potentials and remaining challenges for tree species mapping at the national level. Our findings allow to further improve national-level tree species mapping with medium to high resolution data and provide guidance for similar approaches in other countries where ground-based inventory data are available.

1. Introduction

Spatially explicit and fine-scale information on tree species distribution plays an important role for sustainable forest management, carbon monitoring, conservation, and biodiversity (Gamfeldt et al., 2013; Lehtomäki et al., 2015; Vihervaara et al., 2017), for developing

* Corresponding author at: Thünen Institute of Forest Ecosystems, Alfred-Moeller-Straße 1, 16225 Eberswalde, Germany.
E-mail addresses: lukas.blickensdoerfer@thuenen.de (L. Blickensdörfer), katja.oehmichen@thuenen.de (K. Oehmichen), dirk.pflugmacher@geo.hu-berlin.de (D. Pflugmacher), birgit.kleinschmit@tu-berlin.de (B. Kleinschmit), patrick.hostert@geo.hu-berlin.de (P. Hostert).

https://doi.org/10.1016/j.rse.2024.114069
Received 19 December 2023; Received in revised form 14 February 2024; Accepted 18 February 2024
Available online 24 February 2024

climate adaptation strategies (Hof et al., 2017), and for improving earth system models (Pongratz et al., 2018). In many countries forest species composition is estimated regularly using sample-based forest inventories (Tomppo et al., 2010). However, forest inventories are only conducted in multi-year time intervals. They also do not provide spatially explicit wall-to-wall information.

Remote sensing data are an important source to map forest attributes such as tree species (Holzwarth et al., 2020). During recent years, the multispectral Sentinel-2 (S2) satellites moved into the focus of large-scale analysis and monitoring of land cover (Phiri et al., 2020; Xu et al., 2022). Designed to provide global coverage with short revisit times of 6 days (often better for Central European conditions) and a spatial resolution of up to 10 m (Drusch et al., 2012), they provide the imagery for consistent time series analysis. This is critical for analyzing vegetated land cover, since the high temporal resolution captures seasonal vegetation dynamics associated with phenology and land management (Kowalski et al., 2020; Meroni et al., 2021; Tian et al., 2021). S2 time series have been successfully used in the agricultural domain, for example for crop type mapping (Blickensdörfer et al., 2022; Csillik et al., 2019; Ghassemi et al., 2022), grassland drought monitoring and mowing detection (Kowalski et al., 2023; Schwieder et al., 2022) or fruit tree delineation (Abubakar et al., 2023). S2 time series have also advanced forest applications, e.g., the mapping of tree species (Hemmerling et al., 2021; Kollert et al., 2021) and understory plant communities in deciduous forest (Yang et al., 2023). Hemmerling et al. (2021) mapped tree species across a federal state in Germany. They demonstrated the utility of dense phenological time series for distinguishing nine main tree species. While past studies have shown the potential of S2 time series for tree species mapping, they have been confined to relatively small areas and therefore environmental and phenological gradients. It remains to be seen how well time-series based approaches apply to mapping tree species at the national scale.

Combining data from synthetic-aperture radar (SAR) sensors and multispectral sensors has been shown to improve land cover mapping (Inglada et al., 2016; Prudente et al., 2022; Reiche et al., 2018; van Tricht et al., 2018). Both sensor types collect complementary surface information. Multispectral reflectance is influenced by vegetation physiology and biochemistry, while the signal from SAR is sensitive to vegetation structure and moisture. Further, SAR data are not dependent on clear-sky conditions and solar illumination, and therefore may be useful for augmenting optical observations in cloudy regions. The Sentinel-1 (S1) C-band systems provide SAR data with unprecedented combined high spatial and temporal resolution (5–20 m and 5-day revisit time; Torres et al., 2012). The synergy of the two S1 sensors was exploited successfully for mapping land cover (Venter and Sydenham, 2021) and crop types (Blickensdörfer et al., 2022; Ghassemi et al., 2022). For forest attribute mapping, the benefit of combining S2 and S1 has been demonstrated on smaller test sites (Lechner et al., 2022; Liu et al., 2023). Bjerreskov et al. (2021) mapped forest cover, type, and species for a larger area – the Danish state territory. However, they used biannual composites and therefore did not harness the full potential of the high temporal resolution of the two sensors. The literature shows that complementing optical S2 time series with S1 data can improve tree species mapping, but the potential that lies in their combined, high spatial and temporal resolution has not been exploited, yet.

Forest inventory data are a great source for training classification and regression models with remote sensing data, and they are frequently used in forest attribute mapping (Adams et al., 2020; Ahlswede et al., 2023; Breidenbach et al., 2021; Shang et al., 2020). Generally, two types of inventory data can be distinguished: stand-level inventories and plot-based inventories. Stand-level inventories collect aggregated forest statistics at the level of individual forest stands (polygons). Studies have used stand-level inventory data for mapping tree species with S2 or Landsat data (Grabska et al., 2019; Hemmerling et al., 2021; Hermosilla et al., 2022; Immitzer et al., 2019). Because geolocation of individual trees or even groups of trees within stand-level data is not possible, such studies are restricted to analyzing and reporting classification accuracy for larger pure, single-species stands. In comparison, plot-level inventories have several advantages. They are based on a probability sampling design (Lawrence et al., 2010), which is important for estimating area and map accuracy (Olofsson et al., 2014), and the spatial sampling units (plots) are referenced with global navigation satellite system (GNSS) coordinates. Thus, plot-level inventories are more easily matched with satellite data. However, an inventory plot may still contain a mixture of species. Since excluding plots may lead to biases, ways need to be found to also include mixed plots when training and validating tree species maps.

The use of pure, single-species reference data for model training represents a simplification of the forest landscape and likely limits the generalizability of classification models for more complex landscapes with mixed-species compositions (Fassnacht et al., 2016). This is a common limitation shared and discussed in multiple recent studies (Grabska et al., 2020; Hemmerling et al., 2021; Immitzer et al., 2019). One way to address this limitation is by combining reference labels from pure-species plots with pseudo-labeled samples from mixed-species forests. Pseudo-labeling is an approach in semi-supervised learning that derives reference class labels for unlabeled data (pixels) using supervised learning trained with the labeled data (Hosseiny et al., 2024; Zhou, 2018). Pseudo-labels with the maximum predictive probability may then be selected for training. Other semi-supervised learning methods use prior knowledge of labeled pixels within a defined neighborhood to select suitable pseudo-labels (Hu et al., 2020; Tan et al., 2015). For example, if the pseudo-label matches the reference label in the pixel's neighborhood, the pseudo-label is more likely to be true. If the pseudo-label is not present in the neighborhood, the confidence in the assigned pseudo-label is low. In this study, we test a similar approach that uses the species occurrence information in the inventory data to constrain the generation of pseudo-labels. This way, we extend the training data set to be more representative of the entire study region.

The issue of using pure reference samples also affects map validation. Since map validation is often based on the same reference data as used for model training, validation is often restricted to locations with pure-species compositions (Fassnacht et al., 2016). Such accuracies are a good measure of the separability of species (Grabska et al., 2019; Hemmerling et al., 2021), but they likely overestimate the true map accuracy since mixture effects and boundary effects are avoided. More precise data at the pixel level are needed to address this limitation. Very high-resolution datasets are one option to derive such information (Fassnacht et al., 2016), but are not widely available for large areas. Plot-based forest inventories provide a means to assess tree species maps against all tree species recorded in the field. Comparing map labels against tree proportions based on field measurements is not trivial. However, such comparisons may provide insights on map performance in heterogeneous and mixed forest areas.

In this study, we present an approach for national tree species mapping based on S1/S2 time series and national forest inventory data to provide a foundation for future consistent European-wide species mapping efforts. We test our approach for the area of Germany using field data from variable-radius plots of the German National Forest Inventory (NFI). Specifically, we address the following research questions:

1. Which accuracies can be achieved on a national scale when combining NFI observations with S1 and S2 time series data and environmental conditions for mapping major tree species groups?
2. How different are the classification accuracies between homogenous pure-species and mixed-species forest stands?
3. How do the mapped species areas compare to NFI-based area estimates?

2. Methods

2.1. Study area

Germany covers a total area of 357,581 km^2, of which 32% is forested (Thünen-Institut, 2014a). The forests are temperate forests dominated by broadleaf species (42%). About 76% are comprised of multiple species, and the remaining 24% are single species stands (Thünen-Institut, 2014b). The most common species belong to the groups (*genus*) spruce (*Picea*), pine (*Pinus*), beech (*Fagus*) and oak (*Quercus*). They are the dominating species in about 29%, 23%, 16%, 9% of the German forests, respectively (Thünen-Institut, 2014c). Environmental conditions cover a large gradient from northern lowland plains, through the central uplands with mountains ranging up to 1500 m a.s.l., to alpine ecosystems in the south (Fig. 1). Continental climate predominates the eastern parts, while western regions are under oceanic influence with less extreme winter and summer temperature (Zöller et al., 2017). The current tree species distributions are partly linked to those environmental conditions (e.g., the larger shares of spruce in higher altitudes of South Germany and in the Central Uplands, Polley et al., 2018). Regional deviations from the potential natural vegetation are also prominent (e.g., vast Scots pine stands in North-East Germany resulting from reforestation campaigns after the Second World War). In temperate forests, the plant phenological cycle is mainly driven by temperature (Hanes et al., 2013). The timing of phenological key events, which are critical for species differentiation (Grabska et al., 2019; Hemmerling et al., 2021; Immitzer et al., 2019), can vary throughout the study area by up to two weeks (Brügger et al., 2003; Kowalski et al., 2020; Templ et al., 2018).

2.2. Sentinel-2 time series

We used all available S2 images with a cloud cover of <90% acquired between March 15th and November 31st of 2017 and 2018, respectively. Image pre-processing was performed in the Framework for Operational Radiometric Correction for Environmental Monitoring (FORCE; Frantz, 2019), including image coregistration (Rufin et al., 2020), cloud and cloud shadow removal (Frantz et al., 2018), atmospheric and topographic correction to surface reflectance and nadir-BRDF reflectance adjustment. The bands with 20 m spatial resolution were sharpened to 10 m using a spectral-only setup of the ImproPhe algorithm (Frantz, 2019; Frantz et al., 2016). We used the bands of the visual (bands 2–4), red edge (5–7), near infrared (8) and short-wave infrared wavelength regions (11−12). In addition, the Normalized Difference Vegetation Index (NDVI; Tucker, 1979) was calculated and included, as it was found to be a reliable and valuable index for tree species classification in previous studies (Bjerreskov et al., 2021; Hemmerling et al., 2021; Immitzer et al., 2018).

The availability of data was highly variable in space and time throughout the study area, depending on cloud coverage and S2 orbit overlaps (Fig. 2). We homogenized the data by interpolating data gaps to consistent 5-day time series using a weighted radial basis convolution function (RBF) filter ensemble with variable kernel widths (σ, Schwieder et al., 2016). This approach was successfully used for a similar study covering the German federal state of Brandenburg (Hemmerling et al., 2021). The different filters of the ensemble were weighted according to the observation density in the kernel window and thereby adapted the degree of smoothing to data availability. After testing different combinations of kernel widths, a set of five kernels was found to generate consistent results for the forested areas in our study region: $\sigma \in \{5, 7, 10, 20, 30\}$.

2.3. Sentinel-1 time series

S1 data was accessed through the German cloud computing platform CODE-DE (Benz et al., 2020). CODE-DE provides monthly backscatter composites of co-polarized (VV) and cross-polarized (VH) data calculated from gamma nought backscatter data. The data was recorded in Interferometric Wide Swath mode with a spatial resolution of 5 m × 20 m. The composites were processed in the Sentinel toolbox (Ground Range Detected border and thermal noise removal, calibration, and terrain correction; Benz et al., 2020). Monthly composites from 2017 and 2018 were included in the analysis and resampled to the 10 m resolution to fit the S2 data structure. In contrast to the S2 time series, we also used winter composites from S1 as cloud cover is not a restricting factor and the SAR signal is sensitive to species-specific, structural differences between seasons (Rüetschi et al., 2018). Based on the composites, we additionally calculated the Radar Vegetation Index (RVI; Nasirzadehdizaji et al., 2019), which is sensitive to vegetation cover and biomass: $RVI = \frac{4*VH}{VH+VV}$, and the cross ratio (CR) of co- and cross-polarized backscatter, which is known to be sensitive to biomass, vegetation water content and forest phenology (Frison et al., 2018; Le Toan et al., 1992; Vreugdenhil et al., 2018): $CR = \frac{VH}{VV}$.

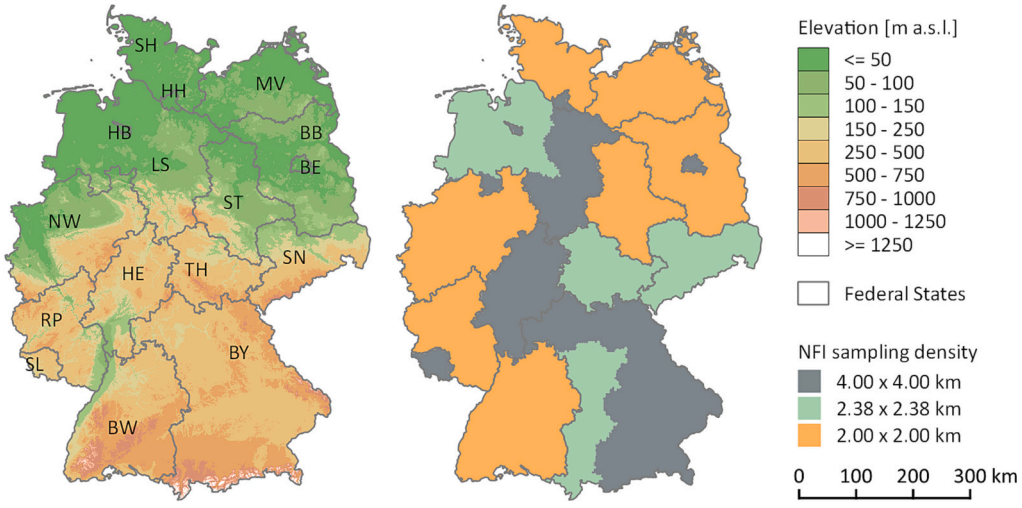

Fig. 1. Overview of Germany's topography (left) and the variation of NFI sampling grid densities (right). Federal States: BW: Baden-Wurttemberg, BY: Bavaria, BE: Berlin, BB: Brandenburg, HB: Bremen, HH: Hamburg, HE: Hesse, LS: Lower Saxony, MV: Mecklenburg-Vorpommern, NW: North Rhine-Westphalia, RP: Rhineland-Palatinate, SL: Saarland, SN: Saxony, ST: Saxony-Anhalt, SH: Schleswig-Holstein, TH: Thuringia. Elevation data: Earth Resources Observation and Science Center (2017).

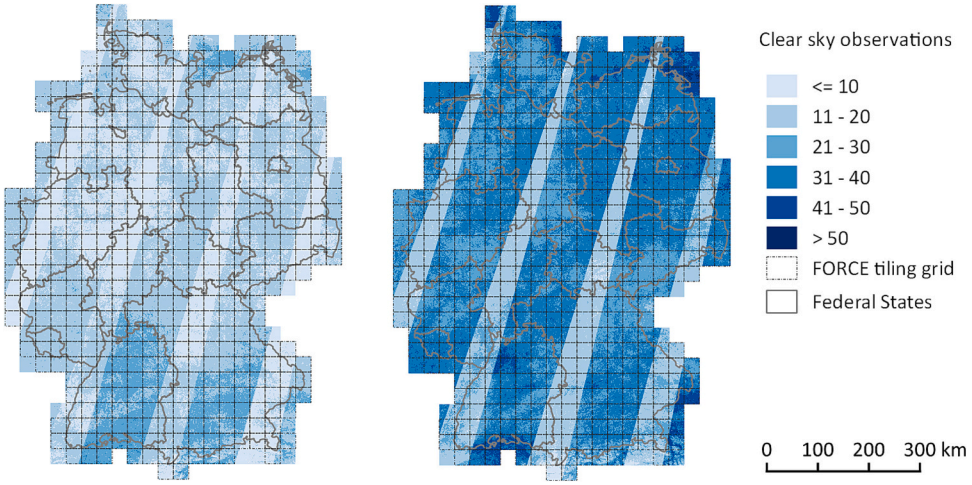

Fig. 2. Number of clear-sky S2 observations per year between March 15th and November 31st (left: 2017, right:2018), superimposed by the FORCE tiling grid of the data cube structure.

2.4. Environmental data

Spectral and temporal characteristics in the S2 and S1 time series differ by tree species and enable species differentiation. However, the diversity of environmental factors throughout the study area can create considerable variation within classes. Annual meteorological conditions steer tree growth and phenology (Brügger et al., 2003), which are physical traits captured by the remote sensing signal. At the same time, long term environmental conditions are key determinants for species distribution (Dyderski et al., 2018). Thus, including variables describing the environmental gradients of the study area as predictors can improve species separability (Grabska et al., 2020; Hościło and Lewandowska, 2019). In this study, we compiled a comprehensive dataset on topographic, climate, meteorological and soil variables, which were input as predictors to the classification algorithm (Table 1). To characterize long-term environmental conditions, we used data on seasonal mean air temperature and precipitation (1981–2010) with a spatial resolution of 1 km × 1 km (DWD, Deutscher Wetterdienst, 2018d; DWD, Deutscher Wetterdienst, 2018e). To describe intra-annual conditions, we included monthly mean temperature, precipitation, and soil moisture content for 2017 and 2018 (DWD, Deutscher Wetterdienst, 2018a, 2018b, 2018c). Local topographic conditions were considered by including elevation, slope and aspect derived from a 10 m × 10 m digital elevation model (DEM; BKG, 2016). Finally, topography induced wetness and water availability was included by deriving the Topographic Wetness Index (TWI) from the DEM ($TWI = ln\left[\frac{A}{tan(\beta)}\right]$, with A being the specific catchment area at the location of interest and β the local slope angle, Gruber and Peckham, 2009).

2.5. National forest inventory

Reference data for this study were derived from the German NFI conducted in 2011/2012. The NFI surveys a total of 59,839 field plots within forest to provide information on forest area, condition, diversity, and production potential at the national scale (Riedel et al., 2017). The survey is based on a permanent cluster sample using a systematic sampling grid with three strata of different sampling density (Fig. 1). It is repeated every ten years, but a sub-sample is recorded every five years based on a reduced set of inventory variables for the national carbon inventory. Each cluster consists of four inventory plots spaced 150 m apart. At each inventory plot numerous variables are recorded regarding individual trees, forest structure and composition, forest habitat types, and dead wood

Surveyed trees are selected through variable-radius sampling

Table 1
Overview of predictor variables included as predictor for machine learning in the analysis.

Variable [unit]	Spatial resolution	Temporal resolution (Observations per year)	Source
Sentinel-2			
blue (band 2) [%] green (3) [%] red (4) [%] red-edge (5–7) [%] near-infrared (8) [%] short-wave infrared (11,12) [%] NDVI [−]	10 m	5-day interpolated (55 per band; 15th Mar. – 31st Nov.)	Own processing; Frantz (2019)
Sentinel-1			
VV [dB] VH [dB]	10 m	monthly composites (12 per band)	Benz et al. (2020)
CR [−] RVI [−]	10 m	monthly composites (12 per index)	Calculated based on Benz et al. (2020)
Topography			
altitude [m]	10 m	constant (1)	BKG (2016)
slope [°]	10 m	constant (1)	Calculated based on BKG (2016)
aspect [°]	10 m	constant (1)	Calculated based on BKG (2016)
TWI [−]	10 m	constant (1)	Calculated based on BKG (2016)
Climate			
temperature [°C]	1 km	seasonal (4)	DWD (2018e)
precipitation [mm]	1 km	seasonal (4)	DWD (2018d)
Meteorology and soil			
temperature [°C]	1 km	monthly (9; Mar. – Nov.)	DWD (2018b)
precipitation [mm]	1 km	monthly (9; Mar. – Nov.)	DWD (2018a)
soil moisture [% NFK]	1 km	monthly (9; Mar. – Nov.)	DWD (2018c)

(Bitterlich, 1984). Here, a tree's sampling probability is proportional to its basal area (defined through the diameter at breast height, DBH, being 1.3 m). The opening angle, defined by the basal area factor (BAF), can be adjusted to increase or decrease the number of trees included in the sample (Fig. 3). Hence, variable-radius plots have no distinct extent and shape. In the NFI, tree species, tree position relative to the plot center and DBH of individual trees, are recorded for a small sample of trees selected through variable-radius sampling with a BAF of four (in the following this sample is referred to as VRS-4). However, VRS-4 tree locations cannot be linked to remote sensing data due to the small number of selected trees and the uncertainty in positional accuracy of the GNSS measurement of the center coordinate (Hogland and Affleck, 2019). Centered on the same point, the species composition of trees higher than 4 m and part of the main forest cover is recorded through a variable-radius sample with a BAF of one or two, depending on tree density (in the following this sample is referred to as VRS-1). This means, VRS-1 includes more trees than VRS-4, however their individual position and DBH are not recorded. We selected the VRS-1 as our reference as it consists of a larger sample of trees, which reduces the uncertainty related to positional accuracy (Hogland and Affleck, 2019; Stehman and Wickham, 2011). We use the term dominant species for the species with the largest basal area share in the VRS-1.

To extract S1/2 pixels associated with each variable-radius plot, we estimated the ground area of each plot by calculating the plot radius associated with the largest tree: $r = \frac{D}{2*\sqrt{BAF}}$, where r is the plot radius, *BAF* is the basal area factor used in VRS-1, and *D* is the largest DBH recorded in VRS-4. In the following, we refer to the estimated plot area as reference plot. We used these reference plots to select reference pixels for training and validating the tree species classification models and the VRS-1 observations as reference labels. On average, reference plots covered 18 S1/2 pixels. Plot diameters ranged between 9 m (2 pixels) and 41 m (47 pixels) for 90% of the reference plots.

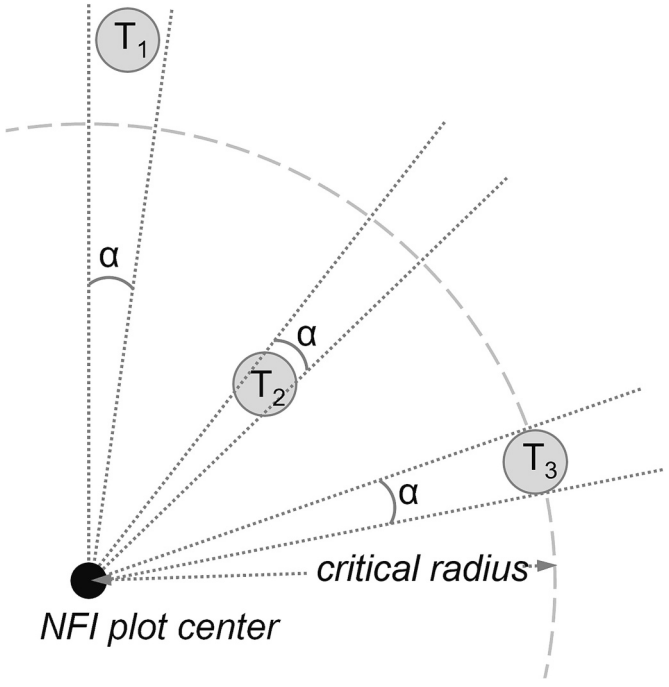

Fig. 3. Schematic representation of the variable-radius sampling method (not to scale). For a survey with an opening angle α (dependent on the chosen BAF), only trees wider than the angle opening are included: T_1, T_2 and T_3 represent trees with equal DBH. T_1 is excluded from the sample while T_2 is included. T_3 is located at the furthest distance to the plot center to still be part of the sample and is displayed to represent the reference plot radius for the given DBH and opening angle α. *Own figure after* Zöhrer (1973).

2.6. Species classification

We followed the species grouping of the NFI to develop a tree species classification comprising eleven classes. The classification differentiates four evergreen coniferous classes (spruce *(Picea)*, pine *(Pinus)*, Douglas fir *(Pseudotsuga menziesii)*, fir *(Abies)*), one deciduous coniferous class (larch *(Larix)*), and four deciduous broadleaf classes (beech *(Fagus)*, oak *(Quercus)*, other deciduous trees with high life span (ODH), and other deciduous trees with low life span (ODL)). We further included birch *(Betula)* and alder *(Alnus)* due to their high area shares at regional level, as separate classes from the ODL group (> 5%, birch in Mecklenburg-Vorpommern, Lower Saxony, Saxony, and Schleswig-Holstein, alder in Mecklenburg-Vorpommern and Schleswig-Holstein, Thünen-Institut, 2014e). In Germany, the number of tree species in each genus is relatively low (Table 2). The spruce, pine, and beech genera are represented by a single species for ≥98% of their area. The *Quercus* genus consists mostly of two species that have about equal area shares (*Quercus robur* and *Quercus pubescens*). Also, the less common tree genera are dominated by single species: fir (*Abies alba*, 95%), alder (*Alnus glutinosa*, 91%), birch (*Betula pendula*, 90%) and larch (*Larix decidua*, 73%). Against this background, we hereafter refer to the listed genera and species groups as tree species to improve readability.

Since there is a time lag of six years between the NFI survey (2011/2012) and the satellite data acquisitions (2017/2018), we removed all NFI plots that may have been disturbed or harvested during that time. To identify these NFI plots, we used the disturbance map by Senf and Seidl

Table 2
Sample size and basal area shares per species group for the training and validation of pure species stands and all stands (pure and mixed-species stands combined, Thünen-Institut, 2014e). * multiple *Populus* and *Salix* Species with area shares <0.5% make up the ODL class and are summarized under their genus for clarity.

Class name	Tree species (>0.5% area share)	Number of NFI plots for training		Number of NFI plots for validation	
		Pure-species plots	Mixed-species plots	Pure-species plots for pixel-based validation	All-species plots for plot-based validation
Pine	*Pinus sylvestris* (22,9%)	3323	925	8738	9499
Spruce	*Picea abies* (31,4%)	3280	1019	6623	8777
Douglas fir	*Pseudotsuga menziesii* (2,0%)	434	81	202	793
Fir	*Abies alba* (2,0%)	210	49	93	970
Larch	*Larix decidua* (1,9%) *Larix kaempferi* (0,7%)	264	99	115	726
Beech	*Fagus sylvatica* (15,1%)	2960	845	1472	7172
Oak	*Quercus robur* (4,5%) *Quercus pubescens* (4,4%)	1265	253	563	4248
Birch	*Betula pendula* (2,1%)	395	151	173	691
Alder	*Alnus glutinosa* (2,6%)	509	26	229	745
ODH	*Fraxinus excelsior* (1,9%) *Carpinus betulus* (1,4%) *Acer pseudoplatanus* (1,5%)	408	64	171	2127
ODL	*Populus* * (0,9%) *Salix* * (< 0.5%)	176	11	52	398

(2020) and excluded all plots that were affected by a stand replacing disturbance after 2011 (severity value threshold by Senf and Seidl, 2020 > 50%). For training the species classification model, we used a random selection of 2/3 of remaining NFI sample clusters.

A common approach is to use samples from pure-species forest stands for training the classification models (Axelsson et al., 2021; Bjerreskov et al., 2021; Persson et al., 2018; Wessel et al., 2018). This can lead to an unbalanced training data set, underrepresenting less-dominant species that mostly occur as minor admixtures in mixed forest. To increase the training sample size and representativeness for those underrepresented species, we developed an approach that creates pseudo-reference class labels for pixels at mixed inventory plots. As the pseudo-labels are used to enlarge the training data set, it is important that labels are assigned with high confidence. Similar to some semi-supervised approaches (Hu et al., 2020; Tan et al., 2015), we leveraged prior knowledge about the pixel neighborhood to increase the confidence in the assigned pseudo-label. Specifically, we used the NFI plot information to constrain pseudo-label generation to locations with specific species distributions. While discriminating multiple tree species in remote sensing data is complex, it is reasonable to assume that deciduous and evergreen species can be distinguished with high accuracy, given their spectral reflectance and different phenological behavior. Therefore, we only considered mixed-species plot locations with two tree species in our approach: one deciduous species and one evergreen species. Assigning pseudo-labels to pixels in selected mixed-species plots was conducted in two steps (Fig. 4): First, we used the training samples (central pixel of NFI plot) from single-species plots - where the dominant species occupied >80% of the basal area in the VRS – to build binary random forest classification models (Breiman, 2001) for the existing two-species admixtures. Each model was trained with a single deciduous species and a single evergreen species to ensure high classification confidence. In a second step, we then applied these models to assign one of the two corresponding tree species classes to pixels within the respective two-species mixed reference plots. After this, each pixel within the respective reference plots has a pseudo label containing a single species class. All pixels with a random forest confidence >75% were then selected as additional training samples. We combined these training samples derived from mixed plots (Table 2, mixed-species plots) with the training samples from pure species plots (Table 2, Pure-species plots) to train the final tree species classification model to map all eleven classes.

We used a random forest classifier as it is insensitive to overfitting and able to handle high-dimensional data with multiple correlated features (Belgiu and Drăguţ, 2016; Breiman, 2001). It essentially includes a variable selection in the process of building the individual decision trees (Breiman, 2001; Lyons et al., 2018; Meyer and Pebesma, 2021). Therefore, all classification models used the full set of predictors (1240 features, Table 1). Each model was trained with 1000 trees. The number of random features considered at each split was set to the square root of the total number of predictor variables. Class imbalance in the training data set can affect the performance of random forest and result in a skewed predictive probability distribution towards the over-represented class (Maxwell et al., 2018). Therefore, we trained the binary classifiers, which we used in the first step of classifying mixed-species plots, on a balanced sample subset by down-sampling the dominant class to match the sample size of the small class. For training the final classification model, we only down-sampled the pine and spruce classes, for which substantially larger sample sizes were available due to their high share of pure-species plots (Table 2). We down-sampled the pine and spruce class to match the sample size of the third largest class (beech) as this yielded a more balanced classification accuracy.

The species classification was applied to forested areas by using a mask that approximates the NFI definition of stocked forest (Langner et al., 2022): To mask un-stocked areas, Langner et al. (2022) used the tree cover density (TCD) High Resolution Layer (HRL; EEA, 2017) provided through the Copernicus land monitoring service and excluded areas with a TCD value <50%. Further, they excluded trees under non-forest use by excluding agricultural and urban areas through the Forest Additional Support Layer (FADSL) HRL (EEA, 2017) and by only considering areas within the classes *forest*, *bog* and *swamp* within the German digital landscape model (DLM) of 2018 (BKG, 2022). Finally, a minimum mapping unit of 0.25 ha (queen's contiguity) was applied to exclude remaining hedges and groves, which are formally not considered forest.

2.7. Validation

Map accuracy for tree species maps is frequently estimated for single-species stands, as reference data does not resolve single trees or species mixtures with sufficient detail (Grabska et al., 2020; Hemmerling et al., 2021). We expand on this by using the NFI data to estimate map accuracy first for single-species stands, but additionally for the entire forest area, including mixed forest. We used an independent validation sample

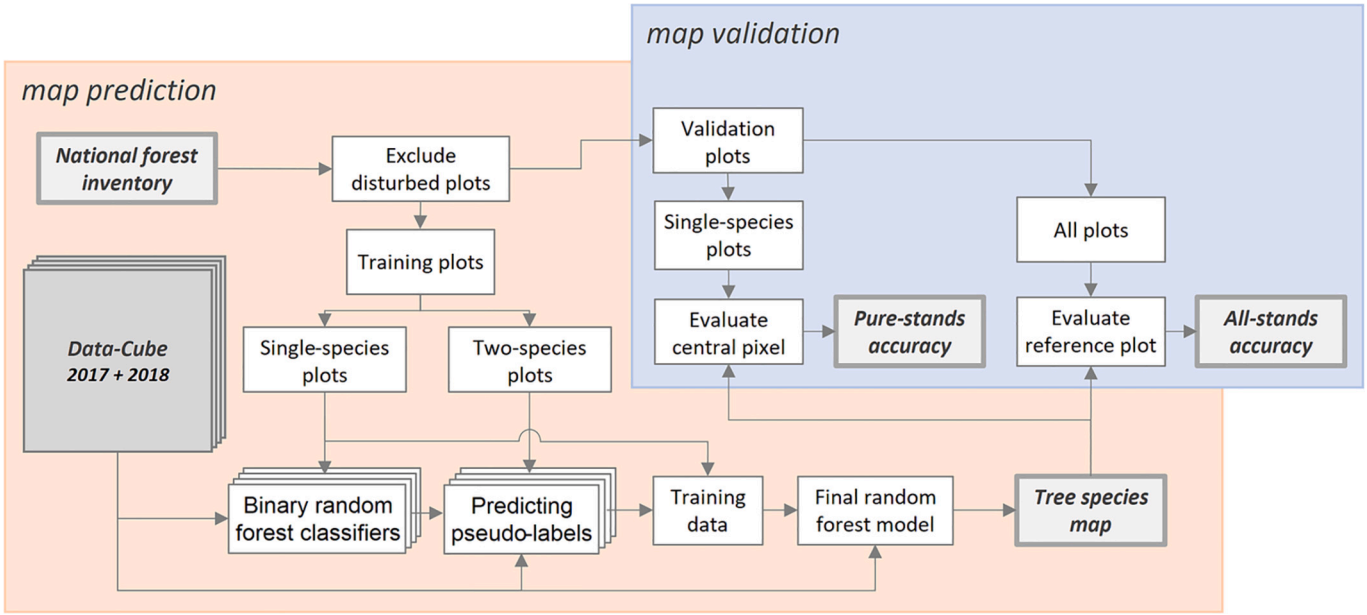

Fig. 4. Classification workflow and map validation. The data-cube contains all preprocessed predictor variables listed in Table 1.

– a random subset of 1/3 of all NFI clusters withhold from model training – to build confusion matrices and estimate overall, user's and producer's accuracies (Congalton, 1991), and F-score (Sokolova and Lapalme, 2009). Accuracy statistics and corresponding standard errors were estimated based on a stratified estimator (Stehman, 2014) that allows the use of separate strata for sampling and estimation, respectively. To estimate map accuracy, the inclusion probability of each sample unit needs to be considered. In our case, the inclusion probability differs with the NFI sampling density. Hence, we used the three regions with common NFI grid spacing as sampling strata (Fig. 1). The map classes served as strata for estimation. To estimate the accuracy of pure-species stands, we used all inventory plots with a dominant species group that accounted for >80% of the total basal area in the VRS-1 (Table 2, Fig. 4). The pixel at the plot center served as sampling unit. In the following, we refer to the resulting accuracy estimates as *pure-stands accuracy*. To estimate the map accuracy including species mixtures, we selected all validation samples (Table 2, Fig. 4). Here, the entire reference plot served as sampling unit (Section 2.5). Reference class labels were assigned according to the species with the largest basal area share in the VRS-1 plot. This approach is also used in the NFI to define the forest stand type of the inventory plots. The map class label was defined as the mode class of all classified pixels within the reference plot. To account for the variable reference plot size when estimating accuracy, each sampling unit received a weight in accordance with its area representation (Stehman and Wickham, 2011). In the following, we call these accuracy estimates *all-stands accuracy*.

In addition to the sample-based accuracy assessment, we assessed the plausibility of the mapped species-specific area at the national and federal state levels. Among many other variables, the NFI evaluation procedure estimates the stocked area shares by leading species and federal state (Thünen-Institut, 2014c), which we compared to area shares for the mapped species. It is important to note that species shares estimated with NFI data are based on basal area as opposed to canopy cover captured by remote sensing.

3. Results

3.1. Pure-stands accuracy

The overall accuracy of pure-species stands was 87.07 ± 0.3%. The two most frequently occurring coniferous species, spruce and pine, were mapped with high accuracies of 90.39 ± 0.31% and 96.63 ± 0.17% (F-score; Table 3). The lower F-score for spruce is a result of a lower producer's accuracy (84.82 ± 0.49%) due to class confusions with Douglas fir and fir along with a higher share of mixed stands, which leads to a slight underestimation of spruce. The two dominant deciduous species, beech and oak, were mapped with F-scores of 88.79 ± 0.57% and 72.64 ± 1.33%, respectively. Here, confusion between the two classes and confusion with ODH results in a slight overestimation of both classes (lower user's accuracy). While alder occupies a smaller area share, it was mapped with equally high accuracy of 82.21 ± 2.29%. These five classes, which were mapped with high accuracy, make up about 92% of the pure-species stands in Germany.

Class-wise accuracies for minor tree species were less balanced indicating either over- or underestimation of their mapped area (Table 3, Fig. 5). For example, producer's accuracy of Douglas fir (86.10 ± 2.63%) and fir (66.33 ± 5.75%) were much higher than their respective user's accuracy (37.07 ± 1.33% and 24.65 ± 1.95%), leading to an overestimation of their area. A similar pattern, however less pronounced, was observed for larch and birch. On the contrary, ODH and ODL were mapped with higher user's accuracy compared to producer's accuracy resulting in an underestimation of area. While those minor species were not mapped accurately, classification errors occurred mostly between physiologically and phenologically similar species (Douglas fir, fir, spruce) or within the broadleaf or coniferous groups (Table 3). Broadleaf and coniferous species, which have pronounced spectral and phenological differences that are captured well within the time-series (Fig. 6), were generally well separated (F-scores of 95.20% and 98.25%, respectively). On the contrary, within the broadleaf group, high spectral-temporal similarity is paired with high within-species variation leading do reduced separability.

A visual assessment of the map confirms the reported accuracy metrics (Fig. 7): homogeneous pure-species stands were mostly classified as one single class and delineated well to neighboring forest stands

Table 3
Confusion matrix for single-species NFI plots to derive pure-stands accuracy. Sample units for accuracy estimation are S1/2 pixels. Cell values indicate percent area. Cells representing over 1% area are highlighted in bold. ODH: Other deciduous trees with high life span; ODL: Other deciduous trees with low life span.

Map class	Reference class (area %)										Σ (%)			Accuracy (%)		
	Pine	Spruce	Douglas fir	Fir	Larch	Beech	Oak	Birch	Alder	ODH	ODL	Map	Ref.	Producer's	User's	F-score
Pine	**33.90**	0.30	0.03	–	0.01	–	0.00	0.07	–	0.00	0.00	34.31	35.84	94.57 ± 0.29	98.79 ± 0.17	96.63 ± 0.17
Spruce	0.51	**29.08**	0.09	0.16	0.00	0.16	0.02	0.02	0.02	0.00	0.00	30.07	34.29	84.82 ± 0.49	96.73 ± 0.29	90.39 ± 0.31
Douglas fir	0.28	**2.21**	**1.57**	0.06	0.00	0.07	0.03	–	0.00	0.00	0.00	4.24	1.83	86.10 ± 2.63	37.07 ± 1.33	51.83 ± 1.39
Fir	0.01	**1.56**	0.09	0.55	–	0.02	0.02	–	–	0.00	0.00	2.25	0.84	66.33 ± 5.75	24.65 ± 1.95	35.94 ± 2.23
Larch	0.29	0.25	0.04	–	**1.01**	0.02	0.03	0.08	–	0.01	0.06	1.78	1.16	87.05 ± 3.39	56.67 ± 2.87	68.64 ± 2.36
Beech	0.06	0.40	0.01	0.03	0.05	**13.09**	0.85	0.09	0.14	0.76	0.08	15.57	13.92	94.07 ± 0.69	84.08 ± 0.85	88.79 ± 0.57
Oak	0.18	0.13	–	–	0.04	0.47	**4.23**	0.22	0.23	0.51	0.23	6.24	5.42	78.17 ± 2.01	67.84 ± 1.75	72.64 ± 1.33
Birch	0.52	0.13	–	0.01	0.03	0.02	0.08	**1.19**	0.05	0.06	0.07	2.17	1.75	68.12 ± 4.38	54.98 ± 2.81	60.85 ± 2.45
Alder	0.03	0.03	–	–	–	0.00	0.01	0.03	**1.66**	0.04	0.05	1.85	2.20	75.73 ± 3.50	89.89 ± 2.39	82.21 ± 2.29
ODH	0.03	0.17	0.00	0.01	0.00	0.04	0.06	0.00	0.08	0.37	0.04	0.82	1.84	20.18 ± 3.48	45.46 ± 5.94	27.95 ± 3.53
ODL	0.04	0.02	0.00	0.00	0.01	0.01	0.07	0.05	0.00	0.10	0.40	0.70	0.93	42.80 ± 7.73	56.77 ± 6.52	48.80 ± 5.57
														Overall accuracy = 87.07 ± 0.3		

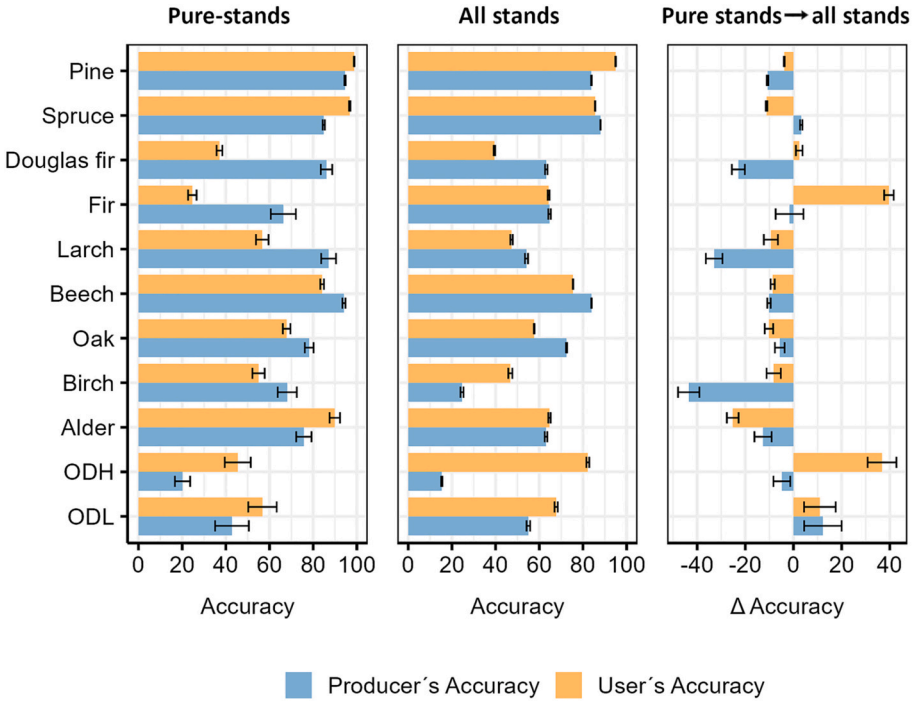

Fig. 5. Metrics for pure-stands accuracy, all-stands accuracy and species-specific differences between pure- and all-stands accuracy. Error bars show the standard error.

(pines in Fig. 7 A/C, Douglas fir and larch in Fig. 7 B/D). Class confusions were mostly observed for minor species. A higher map inconsistency was observed at forest stand borders and in stands with sparse forest cover. Those areas were often falsely classified as larch or birch (Fig. 7 A/C). Species that make up the major share in mixed stands were mostly recognized as such in the map (beech stand in Fig. 7 D), while mixed stands with more balanced species shares were more challenging to classify (Fig. 7 B/D: beech/oak/pine mixed-species stand bordering the larch stand to the south and west).

3.2. *All-stands accuracy*

Including plots from mixed-species stands decreased the estimated map accuracy by 11.5 percentage points (overall accuracy = 75.53 ± 0.07%), compared to the accuracy of pure stands. As observed for pure stands, the major species had a high accuracy (F-score, Table 4): pine (89.05 ± 0.10%), spruce (86.79 ± 0.08%), beech (79.46 ± 0.09%). Oak, the second most frequent deciduous species after beech, achieved an accuracy of 64.22 ± 0.15%. Compared to *pure-stands accuracy*, the confusion of oak with beech and the overestimation within the ODH class was more frequent. The accuracy of larch and birch, which have high shares of mixed-species stands, was lower and reached to F-scores of 50.48 ± 0.43% and 32.27 ± 0.64%, respectively.

The class confusions which dominate the pure stands are in general also driving the error rates in mixed-species forests. For example, high confusion rates between spruce, Douglas fir and fir were observed for pure- and mixed-species stands alike (Table 3, Table 4). However, size and direction of differences between user's and producer's accuracies, especially for minor tree species, vary between pure and mixed stands (Fig. 5). Most notably are differences in user's and producer's accuracy for Douglas fir, larch and birch with reduced producer's accuracy, and for fir and ODH with increased user's accuracy in the all-stands accuracy assessment. The confusion rate between coniferous and deciduous species was higher in mixed stands than in pure-species stands (summarizing species into one broadleaf and one coniferous class archives an F-scores 92.85% for both classes). This confusion between coniferous and deciduous species was mainly observed for beech and spruce, pine and oak, and pine and birch, respectively. Nevertheless, as in pure-species stands, the confusions which make up the largest map area are reported between different broadleaf species (beech, oak, ODH, Table 4).

The comparison of mapped area shares per species with NFI area estimates of the different forest stand types were in line with the pixel- and plot-based accuracy assessment and show a good fit for the main species throughout Germany (Pearson's $r = 0.95$, Fig. 8). At the national level, larger differences between mapped and estimated area exist for the minor species Douglas fir (area overestimated in the map due to confusion with spruce, Table 4) and ODH (underestimated in map due to confusion with beech and oak, Table 4). Overall, the large variety in species composition in federal states is also captured well in the map and a large majority of federal states show correlation coefficients between mapped and NFI area shares of 0.9 or greater. However, regionally dominant forest-stand conditions and structures influenced the respective predicted species area: The challenge to differentiate spruce, Douglas fir and fir, due to their phenological and physiological similarity, affects the respectively predicted area shares. We observed a pronounced overestimation of fir in Baden-Wurttemberg and Douglas fir in Rhineland-Palatinate, causing area underestimation of spruce in both states. The challenge to differentiate broadleaf species, especially when occurring in mixed-species stands, is most apparent in regions with a high share of complex mixed broadleaf-stands (e.g., Rhineland-Palatinate and Saarland with the smallest correlation coefficients of 0.842 and 0.713 respectively; note that the large standard errors for Saarland are due to the small NFI sampling size in the state, Fig. 8). In both states, confusion among broadleaf species resulted in an overestimation of beech.

4. Discussion

In this study, we demonstrated the capability of combining S2, S1, and environmental data with NFI observations to create a national tree species map. Overall and species-specific accuracies of pure-species stands compared well to findings of previous regional studies in temperate forests (Grabska et al., 2020; Hemmerling et al., 2021; Kollert et al., 2021; Welle et al., 2022). Previous work demonstrated the

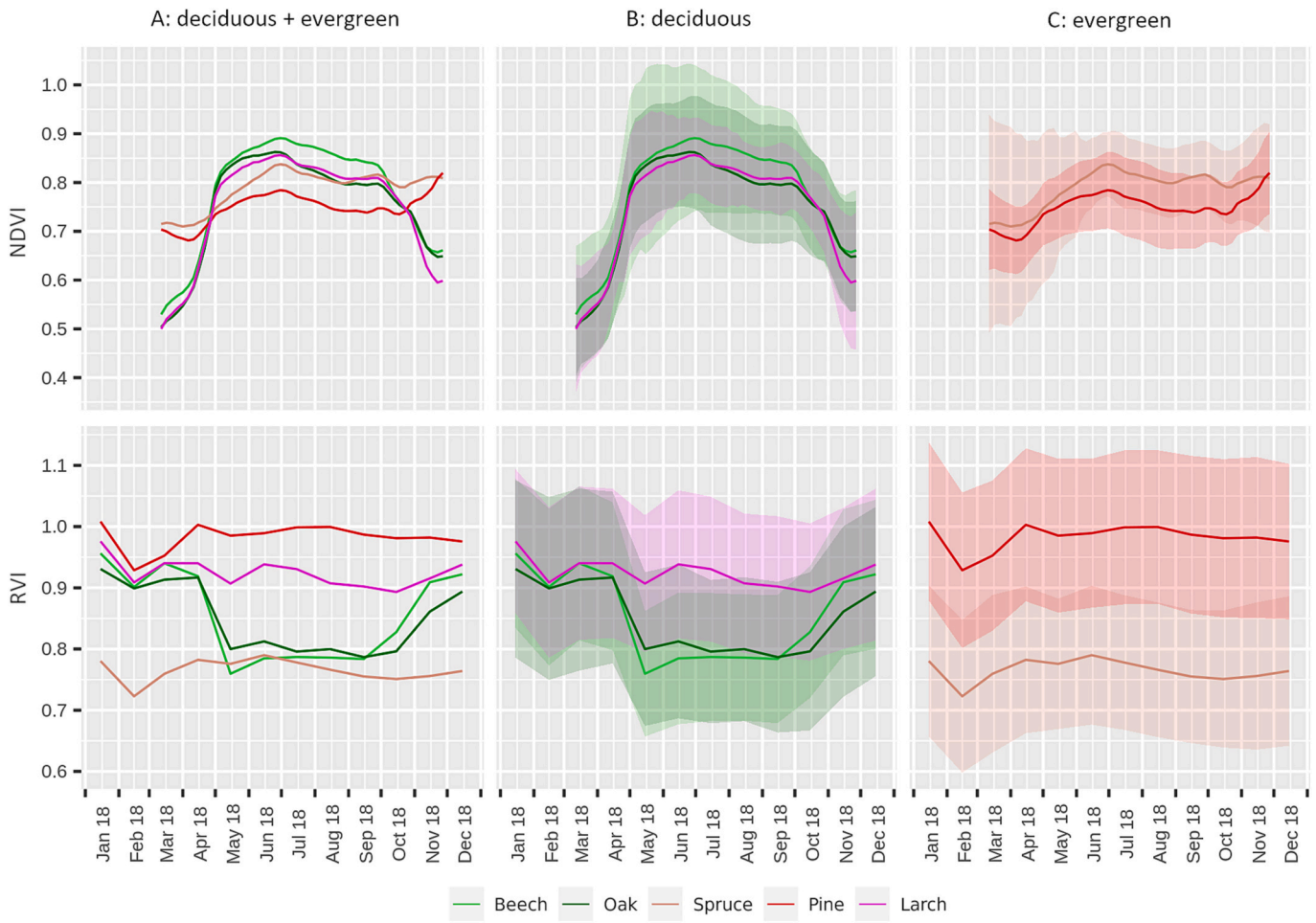

Fig. 6. Mean NDVI and RVI profiles for selected tree species exemplifying spectral-temporal differences between species and within-species variation. Line represents the mean index value for Germany, shaded area represents index range covering 95% of all pure-species reference samples per species (Section 2.5 and 2.6).

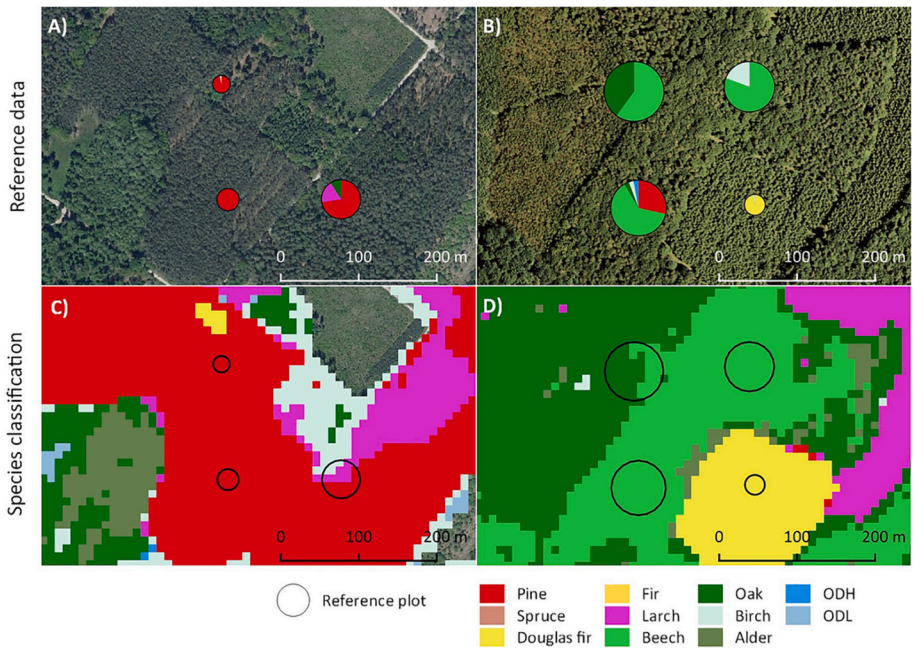

Fig. 7. Tree species classification at NFI plot locations with respective species shares recorded in the NFI displayed in pie charts. The variable size of reference plots stems from the approximation of reference area associated with the variable radius plots (Section 2.5). Note: only three inventory plots are shown in A and C as the fourth plot is located outside of the forest. High Resolution Imagery: Digital Orthophotos, Federal Agency for Cartography and Geodesy, © GeoBasis-DE / BKG, 2022.

Table 4
Confusion matrix for all NFI plots to derive all-stands accuracy. Sample units for accuracy estimation are NFI reference plot areas. The dominant species group at the NFI plot determines the forest stand type, other species are ignored. Cell values indicate percent area. Cells representing over 1% area are highlighted in bold. ODH: Other deciduous trees with high life span; ODL: Other deciduous trees with low life span.

Map class	Reference class (area %)										Σ (%)			Accuracy (%)		
	Pine	Spruce	Douglas fir	Fir	Larch	Beech	Oak	Birch	Alder	ODH	ODL	Map	Ref.	Producer's	User's	F-score
Pine	**14.87**	0.22	0.08	0.00	0.05	0.04	0.12	0.22	0.02	0.01	0.02	15.66	17.74	83.83 ± 0.15	94.96 ± 0.10	89.05 ± 0.10
Spruce	0.74	**22.29**	0.29	0.70	0.19	**1.11**	0.27	0.14	0.12	0.18	0.01	26.04	25.31	88.04 ± 0.10	85.57 ± 0.12	86.79 ± 0.08
Douglas fir	0.46	0.71	**1.42**	0.13	0.08	0.38	0.20	0.10	0.02	0.10	0.02	3.60	2.25	63.21 ± 0.57	39.46 ± 0.35	48.58 ± 0.32
Fir	0.07	0.57	0.13	**1.72**	0.01	0.14	0.00	–	–	0.03	0.00	2.67	2.65	64.70 ± 0.56	64.29 ± 0.41	64.49 ± 0.35
Larch	0.35	0.29	0.03	0.00	**1.03**	0.09	0.25	0.09	0.01	0.01	0.01	2.17	1.90	54.13 ± 0.71	47.29 ± 0.53	50.48 ± 0.43
Beech	0.33	0.81	0.18	0.08	0.19	**21.25**	**2.13**	0.35	0.25	**2.47**	0.12	28.17	25.32	83.92 ± 0.14	75.44 ± 0.12	79.46 ± 0.09
Oak	0.58	0.28	0.08	0.01	0.32	**2.18**	**9.16**	0.55	0.44	**1.93**	0.36	15.89	12.64	72.48 ± 0.24	57.65 ± 0.18	64.22 ± 0.15
Birch	0.21	0.06	0.01	0.01	0.04	0.06	0.12	0.50	0.02	0.04	0.01	1.08	2.04	24.63 ± 0.70	46.76 ± 0.93	32.27 ± 0.64
Alder	0.06	0.06	0.02	0.01	–	0.05	0.27	0.07	**1.52**	0.28	0.01	2.36	2.42	63.08 ± 0.61	64.67 ± 0.53	63.87 ± 0.40
ODH	0.04	0.02	0.00	0.01	0.00	0.03	0.03	0.00	0.00	0.96	0.08	1.17	6.26	15.35 ± 0.30	82.23 ± 0.65	25.86 ± 0.42
ODL	0.02	0.01	0.00	0.00	0.00	0.01	0.07	0.01	0.01	0.25	0.81	1.19	1.47	55.00 ± 0.83	67.72 ± 0.75	60.70 ± 0.59
														Overall accuracy = 75.53 ± 0.07		

capability of S2 time series to accurately separate major species in smaller regions with more narrow environmental gradients, e.g., Hemmerling et al. (2021) for a region in the German lowlands, Grabska et al. (2020) for the Polish Carpathians, and Kollert et al. (2021) for a region in the Austrian Alps. Here we showed that major species can also be mapped well at a national scale, covering a diverse area ranging from alpine environments to low lying planes under oceanic influence.

When mapping tree species over large areas, it is not only important to retrieve a representative reference sample, but also to address the challenge of spectral within-class variability related to the diversity of environmental conditions. We accounted for this variability by including environmental data as explanatory variables in the classification model. Other studies relied on partitioning the study area into temporally fixed subregions and regionalized classification models (Hermosilla et al., 2022; Welle et al., 2022). Such regional models are confined to a smaller environmental variation and, in some cases, a subset of tree species. However, depending on the size of subregions, acquiring sufficient reference data for rare species groups in each subregion can be challenging, if those are distributed throughout the entire study area. Also, using a global model may reduce regional biases introduced by separate models. In this study, we circumvent those problems by presenting a workflow to achieve high map accuracy with a single, global model.

In this study we combined S1 and S2 data for improving tree species classification. Previous research found that dense, interpolated time series are well suited for the homogenization of S2 data for tree species mapping when study area sizes exceed single S2 image tiles and S2 swaths, and cover variable cloud cover conditions (Hemmerling et al., 2021). In our study, the variability in clear-sky observations was substantially higher at the national scale. Thus, we combined cloud cover independent S1 data with the S2 time series to fill potential data gaps. Studies that used only S1 time series data, show that S1 alone can differentiate broadleaf and coniferous trees as well as a few coniferous species (Lechner et al., 2022). Large overlaps of value ranges covered by different species throughout the time series (Fig. 6) exemplify the need of dense temporal information from multiple sensors to capture penological trajectories in the data. To overcome the high image noise and speckle – inherent to S1 images (Moreira et al., 2013) and generated by external factors like moist or snow-covered canopy – we used monthly backscatter composites. This reduces the high temporal observation densities of S1 to improve the signal to noise ratio. Other S1-time series products focus more strongly on the temporal dimension to capture backscatter variation over time, like interferometric repeat-pass coherence (Moreira et al., 2013; Rosen et al., 2000). Those capture vegetation phenology (Villarroya-Carpio et al., 2022) and might provide additional information for species differentiation, but also require more computational resources to derive and additional image preprocessing, like snow masking, to minimize external noise-creating factors. The comparison of an exhaustive set of time-series products from the different sensors was not part of this national scale study, but further research in this direction focusing on S1 data could further improve the information content of the feature set.

To reduce classification bias and to improve the representation of minor species, we developed an approach that extends model training beyond pure-species stands. We adapted the idea from semi-supervised learning approaches that use prior knowledge of the pixel neighborhood (Hu et al., 2020; Tan et al., 2015) to assign pseudo-labels to pixels in mixed forest stands. Ideally, reference samples are collected for fixed areas using precise GNSS data, and for mixed stands, precise reference cover fractions. Moving forward, such reference data could be derived by matching inventory plots to canopy crown segments from very high-resolution imagery (Freudenberg et al., 2022), lidar data (Cao et al., 2023; Ferraz et al., 2016), or both combined. However, such data are in most cases not available for national mapping, yet.

Estimating map accuracy for mixed-species stands is challenging. Therefore, many studies have restricted the map evaluation to pure-species forest stands (Grabska et al., 2019; Hemmerling et al., 2021; Immitzer et al., 2019; Welle et al., 2022). Our study showed that map accuracy substantially decreased if mixed stands were included in the assessment, but the accuracy for major tree species was still acceptable. The decrease in accuracy may have multiple reasons: First, the occurrence of mixed pixels increases in mixed forests and spectral-temporal mixtures of multiple species lead to higher class confusion. Second, geolocation errors in the map and reference data have a stronger effect in mixed stands than in pure-species stands. Increasing the sampling unit from a pixel to a plot when estimating map accuracy for all stands

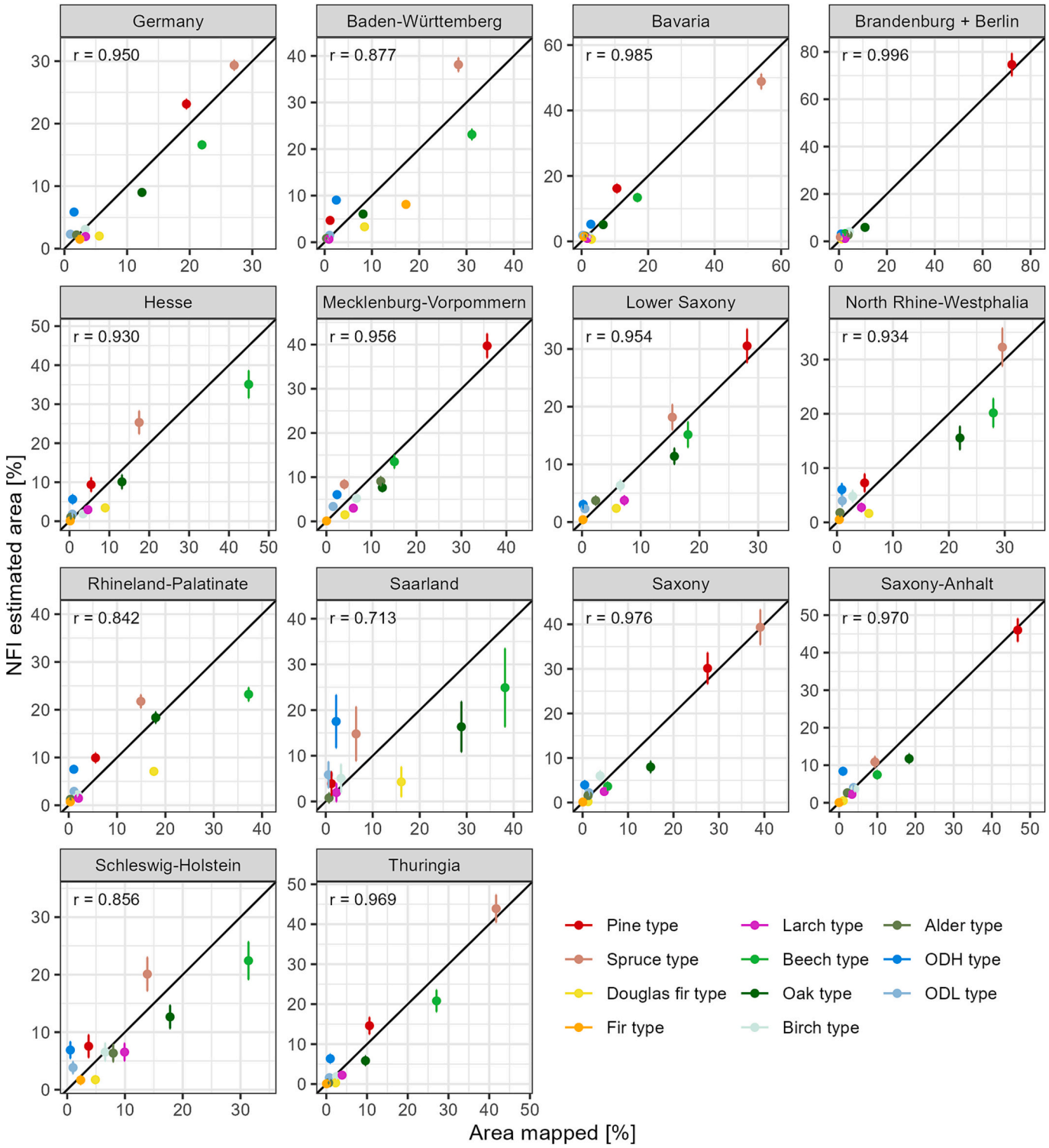

Fig. 8. Mapped area of species groups compared to area estimated for corresponding forest stand types by NFI. Pearson correlation coefficient is denoted by r. Vertical lines represent the 95% confidence interval of the NFI estimate.

(including mixed stands) will likely mitigate some of the uncertainties (Stehman and Wickham, 2011). The pronounced difference between pure-stands and mixed-stands accuracies highlights the need for accuracy assessments that include all forest stands, and identifies mixed, diverse forests as a remaining challenge in tree species classification and starting point for future research.

This study demonstrated the value of NFI data for creating and validating remote sensing based national-scale tree species maps. The large sample sizes and wide range of variables recorded for each sample unit enabled the training of robust species classification models. The systematic sampling grid (Lawrence et al., 2010) allowed for following best practice recommendations for the map accuracy assessment (Olofsson et al., 2014; Stehman and Foody, 2009). Inventory cycles typically stretch over five or ten years, within which countries conduct a periodic complete inventory, or employ an annual or rolling inventory, surveying a subset of plots every year. The definition of the inventory

plot also varies between countries, with concentric circular plots, fixed area plots and variable-radius plots being most common (Gschwantner et al., 2016; Lawrence et al., 2010). In the past, multiple studies already exploited NFI data, e.g., for forest composition and structure mapping in North America (Ohmann and Gregory, 2002), estimation of forest area by tree types in Norway (Breidenbach et al., 2021), and growing stock volume estimation in Italy (Chirici et al., 2020). With increasing availability of Copernicus data (Phiri et al., 2020) and technological advancements in data processing and storage, large-scale, time-series based remote sensing analyses become increasingly accessible for science and for operational use (Woodcock et al., 2020). Looking beyond Germany to the European scale, NFI data, Copernicus image time-series and environmental data are in principle available and can be used to aim at European wide species mapping in future.

To fully exploit the potential of NFI data in remote sensing, a good match between NFI-records and time-series data is crucial. NFI surveying methods were not designed to support or augment remote sensing analyses. Usually, NFI are optimized for the precise and accurate statistical estimation of target variables as well as economic efficiency during data collection. For example, for variable-radius plots, not all trees which contribute to canopy coverage at the sample location are included and surveyed in the NFI. This makes the use of variable radius plots in remote sensing challenging. We chose to use fixed radius plots, but adjusted the radius for each plot dependent on the measured DBH distribution of the respective forest stand. While this did not solve the problem of missing plot geometry, we adjusted the reference plot size to local forest conditions and addressed the dependency of plot extent on DBH distribution. Kirchhoefer et al. (2017) approached this problem by using a high-resolution canopy height model and the relationship between tree height and DBH to model variable-radius sampling tree inclusion for each plot. However, high-resolution canopy height models are rarely available at national or even continental level and results from Kirchhoefer et al. (2017) showed only limited advantage over the use of fixed radius plots. Immitzer et al. (2016) found that combining multiple concentric fixed radius plots with different diameters works well for regression based growing stock estimation at the plot level. This approach remains to be adjusted and tested for pixel-based classification approaches. Looking at potential national applications within and outside Europe, inventory data can vary greatly (Gschwantner et al., 2016; Tomppo et al., 2010) and high-resolution auxiliary data is often not available. The presented approach is flexible enough to fit different inventory plot designs and does not require additional high-resolution data, making it suitable for large-scale application beyond Germany.

The comparison between NFI estimates and species-specific mapped areas showed a strong agreement at the national level and for most subregions. This is an additional indicator of map quality, which can be considered when the data is used in forest monitoring or research. Large-area tree species maps are especially valuable for applications where spatially continuous data is needed that is not provided by sample-based inventories. One example is the economic and ecological assessment of forest disturbance. Multiple remote sensing approaches exist to map forest disturbance (Puhm et al., 2020; Senf and Seidl, 2020; Verbesselt et al., 2012) which can be considered to improve the spatial and temporal resolution of large-scale forest inventories. To characterize disturbed forest areas and assess resulting ecological and economic consequences, species information, among other data on forest attributes, are critical (Thom and Seidl, 2016). In our study, areas of the most common species groups, which make up the major share of harvested timber and are economically most important (Thünen-Institut, 2014d), are captured well in most regions. However, rare species, which contribute to the ecological diversity and resilience (Gang et al., 2023; Thurm et al., 2018), show a larger difference between mapped and NFI-estimated areas in some federal states. This indicates some regional species-specific over- or underestimation. Such inconsistencies between NFI area estimates and the mapped tree species area are mostly related to classification errors. However, some of the observed miss-match might also be caused by differences in definitions. The satellite-based estimates represent crown coverage of tree species in the upper canopy layer (when crown cover is sparse, second layer or undergrowth vegetation adds additional complexity). The leading species per NFI-plot is assigned based on basal area shares by species, which can differ from canopy cover fractions, especially when comparing broadleaf to coniferous species. Therefore, we would expect higher canopy cover fractions for broadleaf trees, and smaller canopy cover fractions for coniferous trees when compared to basal area shares due to the differences in crown shape, which is consistent with our results. We recommend that the insights from national and regional species-specific area comparisons are used in combination with the accuracy assessment to assess the species maps added value for each specific use case.

5. Conclusion

In this study, we present a tree species mapping approach for large areas capable of classifying prominent species with high accuracy, rendering the approach suitable for a wide range of applications. We demonstrated the potential of exploiting all available S2 and S1 data in combination with NFI data as a reference to map the dominant tree species on national scale. First, the suitability of interpolated dense S2 time series data, supplemented with S1 and environmental data, for tree species mapping was confirmed for an area with strong variation in clear-sky observation density. Second, we demonstrated the potential of a large data set designed for statistical sample-based forest inventory to be used in large-scale remote sensing applications, which is promising when considering the large amount of data recorded in NFIs of many countries. Before this background, the presented approach can serve as a steppingstone for tree species mapping efforts at the European scale. Our study also showed the main challenges related to NFI data in the context of remote sensing: the uncertainty in positional accuracy of inventory plot data, inventory methods that are not optimized for remote sensing data analysis, and the small sample sizes for rare species as systematic sampling grids lead to proportional representation of tree species shares. By exploiting the full NFI data set, we also showed, that the remaining challenges for species classification are associated to complex structured mixed-species stands and minor species which predominantly occur as minor admixture alongside dominant species.

Remote sensing-based tree species mapping for large study areas with diverse environmental conditions and forest compositions remains an active field of research. From a remote sensing perspective, further research is needed on how to map mixed-species stands and minor species groups more accurately. In addition, further research on how the long-standing time series of NFI observations can be augmented to facilitate their use in remote sensing data analysis without compromising the independence and integrity of the surveys would be beneficial for a wide range of applications. Such approaches bear the potential to support point-based NFI estimates with wall-to-wall estimates at national scale.

The map of dominant tree species generated in this study is available under: https://atlas.thuenen.de/layers/geonode:Dominant_Species_Class.

CRediT authorship contribution statement

Lukas Blickensdörfer: Writing – original draft, Visualization, Software, Methodology, Investigation, Formal analysis, Data curation, Conceptualization, Writing – review & editing. **Katja Oehmichen:** Writing – review & editing, Supervision, Methodology, Conceptualization, Project administration. **Dirk Pflugmacher:** Writing – review & editing, Methodology, Conceptualization, Writing – original draft. **Birgit Kleinschmit:** Writing – review & editing, Conceptualization. **Patrick Hostert:** Writing – review & editing, Supervision, Conceptualization.

Declaration of competing interest

The authors declare that they have no known competing financial interests or personal relationships that could have appeared to influence the work reported in this paper.

Data availability

Data will be made available on request.

Acknowledgements

This research was funded through a special research funding for greenhouse gas monitoring from the German Federal Ministry of Food and Agriculture. The authors are grateful to the German Federal Agency for Cartography and Geodesy for providing the Digital Landscape Model data, and the European Copernicus Land Monitoring Service for providing the Pan-European High-Resolution Layers. We are grateful to the European Space Agency and the European Commission for making Sentinel-1 and Sentinel-2 data freely available and to CODE-DE for providing the Sentinel-1 monthly mean composites. Our thanks also go to Niklas Langner for processing the forest mask and Marcel Schwieder for assisting with data processing in FORCE. Finally, we would like to thank the anonymous reviewers for their constructive feedback on earlier versions of the article, which helped to improve the manuscript to its final version.

References

Abubakar, M.A., Chanzy, A., Flamain, F., Pouget, G., Courault, D., 2023. Delineation of orchard, vineyard, and olive trees based on phenology metrics derived from time series of Sentinel-2. Remote Sens. (Basel) 15, 2420.

Adams, B., Iverson, L., Matthews, S., Peters, M., Prasad, A., Hix, D.M., 2020. Mapping Forest composition with Landsat time series: An evaluation of seasonal composites and harmonic regression. Remote Sens. (Basel) 12, 610.

Ahlswede, S., Schulz, C., Gava, C., Helber, P., Bischke, B., Förster, M., Arias, F., Hees, J., Demir, B., Kleinschmit, B., 2023. TreeSatAI benchmark archive : a multi-sensor, multi-label dataset for tree species classification in remote sensing. Earth System Science Data 15, 681–695.

Axelsson, A., Lindberg, E., Reese, H., Olsson, H., 2021. Tree species classification using Sentinel-2 imagery and Bayesian inference. International Journal of Applied Earth Observation and Geoinformation 100, 102318.

Belgiu, M., Drăguţ, L., 2016. Random forest in remote sensing: A review of applications and future directions. ISPRS Journal of Photogrammetry and Remote Sensing 114, 24–31.

Benz, U., Banovsky, I., Cesarz, A., Schmidt, M., 2020. CODE-DE portal handbook, Version 2.0. https://code-de.cdn.prismic.io/code-de/ff151913-16e0-4dc3-8005-696bf25bf65d_User+Manual_v2.0.2_ENG.pdf.

Bitterlich, W., 1984. The Relascope Idea. Commonwealth Agricultural Bureaux, Farnham Royal, Slough, England.

Bjerreskov, K.S., Nord-Larsen, T., Fensholt, R., 2021. Classification of Nemoral forests with fusion of multi-temporal Sentinel-1 and 2 data. Remote Sens. (Basel) 13, 950.

BKG, 2016. Digitales Geländemodell Gitterweite 10 m. DGM10, 7 pages. https://sg.geodatenzentrum.de/web_public/gdz/dokumentation/deu/dgm10.pdf (accessed 10 November 2023).

BKG, 2022. Digitales Basis-Landschaftsmodell. Basis-DLM. https://sg.geodatenzentrum.de/web_public/gdz/dokumentation/deu/basis-dlm.pdf (accessed 10 November 2023).

Blickensdörfer, L., Schwieder, M., Pflugmacher, D., Nendel, C., Erasmi, S., Hostert, P., 2022. Mapping of crop types and crop sequences with combined time series of Sentinel-1, Sentinel-2 and Landsat 8 data for Germany. Remote Sens. Environ. 269, 112831.

Breidenbach, J., Waser, L.T., Debella-Gilo, M., Schumacher, J., Rahlf, J., Hauglin, M., Puliti, S., Astrup, R., 2021. National mapping and estimation of forest area by dominant tree species using Sentinel-2 data. Can. J. For. Res. 51, 365–379.

Breiman, L., 2001. Random forests. Mach. Learn. 45, 5–32.

Brügger, R., Dobbertin, M., Kräuchi, N., 2003. Phenological variation of Forest trees. In: Kratochwil, A., Lieth, H., Schwartz, M.D. (Eds.), Phenology: An Integrative Environmental Science. Springer Netherlands, Dordrecht, pp. 255–267.

Cao, Y., Ball, J.G.C., Coomes, D.A., Steinmeier, L., Knapp, N., Wilkes, P., Disney, M., Calders, K., Burt, A., Lin, Y., Jackson, T.D., 2023. Benchmarking airborne laser scanning tree segmentation algorithms in broadleaf forests shows high accuracy only for canopy trees. International Journal of Applied Earth Observation and Geoinformation 123, 103490.

Chirici, G., Giannetti, F., McRoberts, R.E., Travaglini, D., Pecchi, M., Maselli, F., Chiesi, M., Corona, P., 2020. Wall-to-wall spatial prediction of growing stock volume based on Italian National Forest Inventory plots and remotely sensed data. Int. J. Appl. Earth Obs. Geoinf. 84, 101959.

Congalton, R.G., 1991. A review of assessing the accuracy of classifications of remotely sensed data. Remote Sens. Environ. 37, 35–46.

Csillik, O., Belgiu, M., Asner, G.P., Kelly, M., 2019. Object-based time-constrained dynamic time warping classification of crops using Sentinel-2. Remote Sens. (Basel) 11, 1257.

Drusch, M., Del Bello, U., Carlier, S., Colin, O., Fernandez, V., Gascon, F., Hoersch, B., Isola, C., Laberinti, P., Martimort, P., Meygret, A., Spoto, F., Sy, O., Marchese, F., Bargellini, P., 2012. Sentinel-2: ESA's optical high-resolution Mission for GMES operational services. Remote Sens. Environ. 120, 25–36.

DWD, Deutscher Wetterdienst, 2018a. Aktuelle stündlich gleitende RADOLAN-Raster der täglichen Niederschlagshöhe (binär). Version 2.5. https://opendata.dwd.de/climate_environment/CDC/grids_germany/daily/radolan/recent/bin/DESCRIPTION_gridsgermany-daily-radolan-recent-bin_en.pdf (accessed 10 November 2023).

DWD, Deutscher Wetterdienst, 2018b. Grids of monthly averaged daily air temperature (2m) over Germany. version v1.0. https://opendata.dwd.de/climate_environment/CDC/grids_germany/monthly/air_temperature_mean/DESCRIPTION_gridsgermany_monthly_air_temperature_mean_en.pdf (accessed 10 November 2023).

DWD, Deutscher Wetterdienst, 2018c. Monthly grids of soil moisture under grass and sandy loam. version 0.x. http://141.38.2.27/climate_environment/CDC/grids_germany/daily/soil_moist/DESCRIPTION_gridsgermany_daily_soil_moist_en.pdf (accessed 10 November 2023).

DWD, Deutscher Wetterdienst, 2018d. Multi-annual grids of precipitation height over Germany 1981–2010. version v1.0. https://opendata.dwd.de/climate_environment/CDC/grids_germany/multi_annual/precipitation/DESCRIPTION_gridsgermany_multi_annual_precipitation_8110_en.pdf.

DWD, Deutscher Wetterdienst, 2018e. Multi-annual means of grids of air temperature (2m) over Germany 1981–2010. version v1.0. https://opendata.dwd.de/climate_environment/CDC/grids_germany/multi_annual/air_temperature_mean/DESCRIPTION_gridsgermany_multi_annual_air_temperature_mean_8110_en.pdf.

Dyderski, M.K., Paź, S., Frelich, L.E., Jagodziński, A.M., 2018. How much does climate change threaten European forest tree species distributions? Glob. Chang. Biol. 24, 1150–1163.

Earth Resources Observation and Science Center, 2017. Shuttle Radar Topography Mission (SRTM) 1 Arc-Second Global.

EEA, 2017. Copernicus Land Monitoring Service – High Resolution Layer Forest: Product Specifications Document. https://land.copernicus.eu/user-corner/technical-library/forest-2018-user-manual.pdf.

Fassnacht, F.E., Latifi, H., Stereńczak, K., Modzelewska, A., Lefsky, M., Waser, L.T., Straub, C., Ghosh, A., 2016. Review of studies on tree species classification from remotely sensed data. Remote Sens. Environ. 186, 64–87.

Ferraz, A., Saatchi, S., Mallet, C., Meyer, V., 2016. Lidar detection of individual tree size in tropical forests. Remote Sens. Environ. 183, 318–333.

Frantz, D., 2019. FORCE—Landsat + Sentinel-2 analysis ready data and beyond. Remote Sens. (Basel) 11, 1124.

Frantz, D., Stellmes, M., Roder, A., Udelhoven, T., Mader, S., Hill, J., 2016. Improving the spatial resolution of land surface phenology by fusing medium- and coarse-resolution inputs. IEEE Trans. Geosci. Remote Sens. 54, 4153–4164.

Frantz, D., Haß, E., Uhl, A., Stoffels, J., Hill, J., 2018. Improvement of the Fmask algorithm for Sentinel-2 images: separating clouds from bright surfaces based on parallax effects. Remote Sens. Environ. 215, 471–481.

Freudenberg, M., Magdon, P., Nölke, N., 2022. Individual tree crown delineation in high-resolution remote sensing images based on U-net. Neural Comput. & Applic. 34, 22197–22207.

Frison, P.-L., Fruneau, B., Kmiha, S., Soudani, K., Dufrêne, E., Le Toan, T., Koleck, T., Villard, L., Mougin, E., Rudant, J.-P., 2018. Potential of Sentinel-1 data for monitoring temperate mixed Forest phenology. Remote Sens. (Basel) 10, 2049.

Gamfeldt, L., Snäll, T., Bagchi, R., Jonsson, M., Gustafsson, L., Kjellander, P., Ruiz-Jaen, M.C., Fröberg, M., Stendahl, J., Philipson, C.D., Mikusiński, G., Andersson, E., Westerlund, B., Andrén, H., Moberg, F., Moen, J., Bengtsson, J., 2013. Higher levels of multiple ecosystem services are found in forests with more tree species. Nat. Commun. 4, 1340.

Gang, B., Bingham, L., Gosling, E., Knoke, T., 2023. Assessing the suitability of under-represented tree species for multifunctional forest management—an example using economic return and biodiversity indicators. Forestry: An International Journal of Forest Research. cpad038 https://doi.org/10.1093/forestry/cpad038.

Ghassemi, B., Immitzer, M., Atzberger, C., Vuolo, F., 2022. Evaluation of accuracy enhancement in European-wide crop type mapping by combining optical and microwave time series. Land 11, 1397.

Grabska, E., Hostert, P., Pflugmacher, D., Ostapowicz, K., 2019. Forest stand species mapping using the Sentinel-2 time series. Remote Sens. (Basel) 11, 1197.

Grabska, E., Frantz, D., Ostapowicz, K., 2020. Evaluation of machine learning algorithms for forest stand species mapping using Sentinel-2 imagery and environmental data in the polish Carpathians. Remote Sens. Environ. 251, 112103.

Gruber, S., Peckham, S., 2009. Chapter 7 land-surface parameters and objects in hydrology. In: Geomorphometry - Concepts, Software, Applications. Elsevier, pp. 171–194.

Gschwantner, T., Lanz, A., Vidal, C., Bosela, M., Di Cosmo, L., Fridman, J., Gasparini, P., Kuliešis, A., Tomter, S., Schadauer, K., 2016. Comparison of methods used in European National Forest Inventories for the estimation of volume increment: towards harmonisation. Ann. For. Sci. 73, 807–821.

Hanes, J.M., Richardson, A.D., Klosterman, S., 2013. Mesic temperate deciduous Forest phenology. In: Schwartz, M.D. (Ed.), Phenology: An Integrative Environmental Science. Springer Netherlands, Dordrecht, pp. 211–224.

Hemmerling, J., Pflugmacher, D., Hostert, P., 2021. Mapping temperate forest tree species using dense Sentinel-2 time series. Remote Sens. Environ. 267, 112743.
Hermosilla, T., Bastyr, A., Coops, N.C., White, J.C., Wulder, M.A., 2022. Mapping the presence and distribution of tree species in Canada's forested ecosystems. Remote Sens. Environ. 282, 113276.
Hof, A.R., Dymond, C.C., Mladenoff, D.J., 2017. Climate change mitigation through adaptation: the effectiveness of forest diversification by novel tree planting regimes. Ecosphere 8, e01981.
Hogland, J., Affleck, D.L.R., 2019. Mitigating the impact of field and image registration errors through spatial aggregation. Remote Sens. (Basel) 11, 222.
Holzwarth, S., Thonfeld, F., Abdullahi, S., Asam, S., Da Ponte Canova, E., Gessner, U., Huth, J., Kraus, T., Leutner, B., Kuenzer, C., 2020. Earth observation based monitoring of forests in Germany: A review. Remote Sens. (Basel) 12, 3570.
Hościło, A., Lewandowska, A., 2019. Mapping Forest type and tree species on a regional scale using multi-temporal Sentinel-2 data. Remote Sens. (Basel) 11, 929.
Hosseiny, B., Mahdianpari, M., Hemati, M., Radman, A., Mohammadimanesh, F., Chanussot, J., 2024. Beyond supervised learning in remote sensing: A systematic review of deep learning approaches. IEEE Journal of Selected Topics in Applied Earth Observations and Remote Sensing 17, 1035–1052.
Hu, Y., An, R., Wang, B., Xing, F., Ju, F., 2020. Shape adaptive neighborhood information-based semi-supervised learning for hyperspectral image classification. Remote Sens. (Basel) 12, 2976.
Immitzer, M., Stepper, C., Böck, S., Straub, C., Atzberger, C., 2016. Use of WorldView-2 stereo imagery and National Forest Inventory data for wall-to-wall mapping of growing stock. For. Ecol. Manage. 359, 232–246.
Immitzer, M., Böck, S., Einzmann, K., Vuolo, F., Pinnel, N., Wallner, A., Atzberger, C., 2018. Fractional cover mapping of spruce and pine at 1 ha resolution combining very high and medium spatial resolution satellite imagery. Remote Sens. Environ. 204, 690–703.
Immitzer, M., Neuwirth, M., Böck, S., Brenner, H., Vuolo, F., Atzberger, C., 2019. Optimal input features for tree species classification in Central Europe based on multi-temporal Sentinel-2 data. Remote Sens. (Basel) 11, 2599.
Inglada, J., Vincent, A., Arias, M., Marais-Sicre, C., 2016. Improved early crop type identification by joint use of high temporal resolution SAR and optical image time series. Remote Sens. (Basel) 8, 362.
Kirchhoefer, M., Schumacher, J., Adler, P., Kändler, G., 2017. Considerations towards a novel approach for integrating angle-count sampling data in remote sensing based Forest inventories. Forests 8, 239.
Kollert, A., Bremer, M., Löw, M., Rutzinger, M., 2021. Exploring the potential of land surface phenology and seasonal cloud free composites of one year of Sentinel-2 imagery for tree species mapping in a mountainous region. International Journal of Applied Earth Observation and Geoinformation 94, 102208.
Kowalski, K., Senf, C., Hostert, P., Pflugmacher, D., 2020. Characterizing spring phenology of temperate broadleaf forests using Landsat and Sentinel-2 time series. International Journal of Applied Earth Observation and Geoinformation 92, 102172.
Kowalski, K., Okujeni, A., Hostert, P., 2023. A generalized framework for drought monitoring across central European grassland gradients with Sentinel-2 time series. Remote Sens. Environ. 286, 113449.
Langner, N., Oehmichen, K., Henning, L., Blickensdörfer, L., Riedel, T., 2022. Stocked Forest Area Map 2018. https://doi.org/10.3220/DATA20221205151218.
Lawrence, M., McRoberts, R.E., Tomppo, E., Gschwantner, T., Gabler, K., 2010. Comparisons of National Forest Inventories. In: Tomppo, E., Gschwantner, T., Lawrence, M., McRoberts, R.E. (Eds.), National Forest Inventories. Springer Netherlands, Dordrecht, pp. 19–32.
Le Toan, T., Beaudoin, A., Riom, J., Guyon, D., 1992. Relating forest biomass to SAR data. IEEE Trans. Geosci. Remote Sens. 30, 403–411.
Lechner, M., Dostálová, A., Hollaus, M., Atzberger, C., Immitzer, M., 2022. Combination of Sentinel-1 and Sentinel-2 data for tree species classification in a central European biosphere reserve. Remote Sens. (Basel) 14, 2687.
Lehtomäki, J., Tuominen, S., Toivonen, T., Leinonen, A., 2015. What data to use for Forest conservation planning? A comparison of coarse open and detailed proprietary Forest inventory data in Finland. PloS One 10, e0135926.
Liu, X., Frey, J., Munteanu, C., Still, N., Koch, B., 2023. Mapping tree species diversity in temperate montane forests using Sentinel-1 and Sentinel-2 imagery and topography data. Remote Sens. Environ. 292, 113576.
Lyons, M.B., Keith, D.A., Phinn, S.R., Mason, T.J., Elith, J., 2018. A comparison of resampling methods for remote sensing classification and accuracy assessment. Remote Sens. Environ. 208, 145–153.
Maxwell, A.E., Warner, T.A., Fang, F., 2018. Implementation of machine-learning classification in remote sensing: an applied review. International Journal of Remote Sensing 39, 2784–2817.
Meroni, M., d'Andrimont, R., Vrieling, A., Fasbender, D., Lemoine, G., Rembold, F., Seguini, L., Verhegghen, A., 2021. Comparing land surface phenology of major European crops as derived from SAR and multispectral data of Sentinel-1 and -2. Remote Sens. Environ. 253, 112232.
Meyer, H., Pebesma, E., 2021. Predicting into unknown space? Estimating the area of applicability of spatial prediction models. Methods Ecol. Evol. 12, 1620–1633.
Moreira, A., Prats-Iraola, P., Younis, M., Krieger, G., Hajnsek, I., Papathanassiou, K.P., 2013. A tutorial on synthetic aperture radar. IEEE Geoscience and Remote Sensing Magazine 1, 6–43.
Nasirzadehdizaji, R., Balik Sanli, F., Abdikan, S., Cakir, Z., Sekertekin, A., Ustuner, M., 2019. Sensitivity analysis of multi-temporal Sentinel-1 SAR parameters to crop height and canopy coverage. Appl. Sci. 9, 655.
Ohmann, J.L., Gregory, M.J., 2002. Predictive mapping of forest composition and structure with direct gradient analysis and nearest- neighbor imputation in coastal Oregon, U.S.A. Can. J. For. Res. 32, 725–741.
Olofsson, P., Foody, G.M., Herold, M., Stehman, S.V., Woodcock, C.E., Wulder, M.A., 2014. Good practices for estimating area and assessing accuracy of land change. Remote Sens. Environ. 148, 42–57.
Persson, M., Lindberg, E., Reese, H., 2018. Tree species classification with multi-temporal Sentinel-2 data. Remote Sens. (Basel) 10, 1794.
Phiri, D., Simwanda, M., Salekin, S., Nyirenda, V., Murayama, Y., Ranagalage, M., 2020. Sentinel-2 data for land cover/use mapping: A review. Remote Sens. (Basel) 12, 2291.
Polley, H., Hennig, P., Kroiher, F., Marks, A., Riedel, T., Schmidt, U., Schwitzgebel, F., Stauber, T., 2018. Der Wald in Deutschland. Ausgewählte Ergebnisse der dritten Bundeswaldinventur, Berlin. https://www.bmel.de/SharedDocs/Downloads/DE/Broschueren/bundeswaldinventur3.pdf (accessed 13 November 2023).
Pongratz, J., Dolman, H., Don, A., Erb, K.-H., Fuchs, R., Herold, M., Jones, C., Kuemmerle, T., Luyssaert, S., Meyfroidt, P., Naudts, K., 2018. Models meet data: challenges and opportunities in implementing land management in earth system models. Glob. Chang. Biol. 24, 1470–1487.
Prudente, V.H.R., Skakun, S., Oldoni, L.V., Xaud, A.M., Xaud, M.R., Adami, M., Sanches, I.D., 2022. Multisensor approach to land use and land cover mapping in Brazilian Amazon. ISPRS Journal of Photogrammetry and Remote Sensing 189, 95–109.
Puhm, M., Deutscher, J., Hirschmugl, M., Wimmer, A., Schmitt, U., Schardt, M., 2020. A near real-time method for Forest change detection based on a structural time series model and the Kalman filter. Remote Sens. (Basel) 12, 3135.
Reiche, J., Hamunyela, E., Verbesselt, J., Hoekman, D., Herold, M., 2018. Improving near-real time deforestation monitoring in tropical dry forests by combining dense Sentinel-1 time series with Landsat and ALOS-2 PALSAR-2. Remote Sens. Environ. 204, 147–161.
Riedel, T., Hennig, P., Kroiher, F., Polley, H., Schmitz, F., Schwitzgebel, F., 2017. Die dritte Bundeswaldinventur BWI 2012. Inventur- und Auswertungsmethoden. Johann Heinrich von Thünen–Institut, Bundesforschungsinstitut für Ländliche Räume, Wald und Fischerei. Thünen-Institut für Waldökosysteme, Berlin. https://bwi.info/Download/de/Methodik/BMEL_BWI_Methodenband_Web_BWI3.pdf (accessed 13 November 2023).
Rosen, P.A., Hensley, S., Joughin, I.R., Li, F.K., Madsen, S.N., Rodriguez, E., Goldstein, R. M., 2000. Synthetic aperture radar interferometry. Proc. IEEE 88, 333–382.
Rüetschi, M., Schaepman, M., Small, D., 2018. Using multitemporal Sentinel-1 C-band backscatter to monitor phenology and classify deciduous and coniferous forests in northern Switzerland. Remote Sens. (Basel) 10, 55.
Rufin, P., Frantz, D., Yan, L., Hostert, P., 2020. Operational Coregistration of the sentinel-2A/B image archive using multitemporal Landsat spectral averages. IEEE Geosci. Remote Sens. Lett. 1–5.
Schwieder, M., Leitão, P.J., Bustamante, Cunha, Maria, Mercedes, Ferreira, L.G., Rabe, A., Hostert, P., 2016. Mapping Brazilian savanna vegetation gradients with Landsat time series. International Journal of Applied Earth Observation and Geoinformation 52, 316–370.
Schwieder, M., Wesemeyer, M., Frantz, D., Pfoch, K., Erasmi, S., Pickert, J., Nendel, C., Hostert, P., 2022. Mapping grassland mowing events across Germany based on combined Sentinel-2 and Landsat 8 time series. Remote Sens. Environ. 269, 112795.
Senf, C., Seidl, R., 2020. Mapping the forest disturbance regimes of Europe. Nature Sustainability. 4, 63–70.
Shang, C., Coops, N.C., Wulder, M.A., White, J.C., Hermosilla, T., 2020. Update and spatial extension of strategic forest inventories using time series remote sensing and modeling. International Journal of Applied Earth Observation and Geoinformation 84, 101956.
Sokolova, M., Lapalme, G., 2009. A systematic analysis of performance measures for classification tasks. Inf. Process. Manag. 45, 427–437.
Stehman, S.V., 2014. Estimating area and map accuracy for stratified random sampling when the strata are different from the map classes. Int. J. Remote Sens. 35, 4923–4939.
Stehman, S.V., Foody, G.M., 2009. Accuracy assessment. In: Warner, T.A., Nellis, M.D., Foody, G.M. (Eds.), The SAGE Handbook of Remote Sensing. SAGE, Los Angeles, Calif, pp. 297–310.
Stehman, S.V., Wickham, J.D., 2011. Pixels, blocks of pixels, and polygons: choosing a spatial unit for thematic accuracy assessment. Remote Sens. Environ. 115, 3044–3055.
Tan, K., Hu, J., Li, J., Du, P., 2015. A novel semi-supervised hyperspectral image classification approach based on spatial neighborhood information and classifier combination. ISPRS J. Photogramm. Remote Sens. 105, 19–29.
Templ, B., Koch, E., Bolmgren, K., Ungersböck, M., Paul, A., Scheifinger, H., Rutishauser, T., Busto, M., Chmielewski, F.-M., Hájková, L., Hodzić, S., Kaspar, F., Pietragalla, B., Romero-Fresneda, R., Tolvanen, A., Vučetič, V., Zimmermann, K., Zust, A., 2018. Pan European Phenological database (PEP725): a single point of access for European data. Int. J. Biometeorol. 62, 1109–1113.
Thom, D., Seidl, R., 2016. Natural disturbance impacts on ecosystem services and biodiversity in temperate and boreal forests. Biol. Rev. Camb. Philos. Soc. 91, 760–781.
Thünen-Institut, 2014a. Third National Forest Inventory - Results Database. Forest area [ha] by Land and accessibility, Filter: year=2012 (77Z1JI_L101of_2012). https://bwi.info (accessed 15 November 2023).
Thünen-Institut, 2014b. Third National Forest Inventory - Results Database. Forest area [ha] by Land and admixture, Filter: year=2012 (69Z1JI_L321of_2012_L322). https://bwi.info (accessed 15 November 2023).
Thünen-Institut, 2014c. Third National Forest Inventory - Results Database. Forest area [ha] by Land and stocking type of main stocking, Filter: Jahr=2012 (69Z1JI_L343of_2012_L344). https://bwi.info (accessed 15 November 2023).

Thünen-Institut, 2014d. Third National Forest Inventory - Results Database. Timber stock (harvestable volume under bark) of used stand [1000 m^3/a] by Land and tree species group. https://bwi.info (accessed 15 November 2023).
Thünen-Institut, 2014e. Third National Forest Inventory - Results Database. Share in basal area [%] by tree species and federal state, Filter: year=2012, (77Z1JI_L296of_2012_bi_Ba). https://bwi.info (accessed 15 November 2023).
Thurm, E.A., Hernandez, L., Baltensweiler, A., Ayan, S., Rasztovits, E., Bielak, K., Zlatanov, T.M., Hladnik, D., Balic, B., Freudenschuss, A., Büchsenmeister, R., Falk, W., 2018. Alternative tree species under climate warming in managed European forests. For. Ecol. Manage. 430, 485–497.
Tian, F., Cai, Z., Jin, H., Hufkens, K., Scheifinger, H., Tagesson, T., Smets, B., van Hoolst, R., Bonte, K., Ivits, E., Tong, X., Ardö, J., Eklundh, L., 2021. Calibrating vegetation phenology from Sentinel-2 using eddy covariance, PhenoCam, and PEP725 networks across Europe. Remote Sens. Environ. 260, 112456.
Tomppo, E., Gschwantner, T., Lawrence, M., McRoberts, R.E., 2010. National Forest Inventories. Springer Netherlands, Dordrecht.
Torres, R., Snoeij, P., Geudtner, D., Bibby, D., Davidson, M., Attema, E., Potin, P., Rommen, B., Floury, N., Brown, M., Traver, I.N., Deghaye, P., Duesmann, B., Rosich, B., Miranda, N., Bruno, C., L'Abbate, M., Croci, R., Pietropaolo, A., Huchler, M., Rostan, F., 2012. GMES Sentinel-1 mission. Remote Sens. Environ. 120, 9–24.
Tucker, C.J., 1979. Red and photographic infrared linear combinations for monitoring vegetation. Remote Sens. Environ. 8, 127–150.
van Tricht, K., Gobin, A., Gilliams, S., Piccard, I., 2018. Synergistic use of radar Sentinel-1 and optical Sentinel-2 imagery for crop mapping: A case study for Belgium. Remote Sens. (Basel) 10, 1642.
Venter, Z.S., Sydenham, M.A.K., 2021. Continental-scale land cover mapping at 10 m resolution over Europe (ELC10). Remote Sens. (Basel) 13, 2301.
Verbesselt, J., Zeileis, A., Herold, M., 2012. Near real-time disturbance detection using satellite image time series. Remote Sens. Environ. 123, 98–108.
Vihervaara, P., Auvinen, A.-P., Mononen, L., Törmä, M., Ahlroth, P., Anttila, S., Böttcher, K., Forsius, M., Heino, J., Heliölä, J., Koskelainen, M., Kuussaari, M., Meissner, K., Ojala, O., Tuominen, S., Viitasalo, M., Virkkala, R., 2017. How essential biodiversity variables and remote sensing can help national biodiversity monitoring. Global Ecology and Conservation 10, 43–59.
Villarroya-Carpio, A., Lopez-Sanchez, J.M., Engdahl, M.E., 2022. Sentinel-1 interferometric coherence as a vegetation index for agriculture. Remote Sens. Environ. 280, 113208.
Vreugdenhil, M., Wagner, W., Bauer-Marschallinger, B., Pfeil, I., Teubner, I., Rüdiger, C., Strauss, P., 2018. Sensitivity of Sentinel-1 backscatter to vegetation dynamics: An Austrian case study. Remote Sens. (Basel) 10, 1396.
Welle, T., Aschenbrenner, L., Kuonath, K., Kirmaier, S., Franke, J., 2022. Mapping dominant tree species of German forests. Remote Sens. (Basel) 14, 3330.
Wessel, M., Brandmeier, M., Tiede, D., 2018. Evaluation of different machine learning algorithms for scalable classification of tree types and tree species based on Sentinel-2 data. Remote Sens. (Basel) 10, 1419.
Woodcock, C.E., Loveland, T.R., Herold, M., Bauer, M.E., 2020. Transitioning from change detection to monitoring with remote sensing: A paradigm shift. Remote Sens. Environ. 238, 111558.
Xu, L., Herold, M., Tsendbazar, N.-E., Masiliünas, D., Li, L., Lesiv, M., Fritz, S., Verbesselt, J., 2022. Time series analysis for global land cover change monitoring: A comparison across sensors. Remote Sens. Environ. 271, 112905.
Yang, X., Qiu, S., Zhu, Z., Rittenhouse, C., Riordan, D., Cullerton, M., 2023. Mapping understory plant communities in deciduous forests from Sentinel-2 time series. Remote Sens. Environ. 293, 113601.
Zhou, Z.-H., 2018. A brief introduction to weakly supervised learning. Natl. Sci. Rev. 5, 44–53.
Zöhrer, F., 1973. Zur Theorie der Winkelzählprobe für die Forstinventur. Forstwissenschaftliches Centralblatt 92, 53–68.
Zöller, L., Beierkuhnlein, C., Faust, D., Samimi, C. (Eds.), 2017. Die physische Geographie Deutschlands. WBG, Darmstadt.